Implied Volatility Modelling

by

Anyi Zhu

A thesis

presented to the University of Waterloo

in fulfilment of the

thesis requirement for the degree of

Master of Quantitative Finance

Waterloo, Ontario, Canada, 2013

I hereby declare that I am the sole author of this thesis. This is a true copy of the thesis, including any required final revisions, as accepted by my examiners.

I understand that my thesis may be made electronically available to the public.

Abstract

We propose extensions on calibrating the volatility surface through multi-factor regression models. The proposed models are back-tested against the historical S&P 500 implied volatilities during both the volatile and non-volatile periods (as indicated by the VIX index during the same period) and the relevant statistics (adjusted R^2-statistics and root-mean-squared-error (RMSE) statistics) are used to assess the fits of the models. Furthermore, both the equal-weighted method and an alternative method by using observed implied volatilities as the weight are deployed and the results produced by the two methods are compared. Finally we also discuss the possibilities of using promptness, instead of time to maturity, in the regression model to better capture the shape of the volatility surface.

Contents

Introduction

Volatility surface has been an active area of research in finance due to its importance in option pricing, particularly in pricing of path-dependent options. The most popular approach for modelling volatility has been the use of the Black-Scholes framework, with the assumption of constant volatility. However, such an assumption is not consistent with the observations in the real market. Several approaches are suggested in this thesis to improve the modelling of volatility surface and parametric representations are adopted using a regression-based approach which is computationally much less intensive.

This thesis explores some of the parametric regression representations suggested by previous studies with the S&P500 index data for specific periods which are characterized by unusually high and low market volatility, as identified by the level of VIX index and fits the volatility surfaces using both the unweighted and weighted methods using observed implied volatility as the weight. Finally, the thesis also provides some discussions on using the concept of promptness instead of time to maturity as a factor in the parametric regression models.

The remaining structure of this thesis is organized as follows.

Chapter 1 provides background knowledge of options as financial derivatives as well as types of options that are being traded and priced in the financial markets today. Then we have a brief discussion on the classic Black-Scholes model, focusing the underlying assumptions and its limitations. Lastly, the ideas of local volatility and stochastic volatility, as a natural progression of the idea of constant volatility, are discussed in the context of continuous-time framework.

Chapter 2 outlines some recent areas of volatility modelling as described by Homescu [18], namely:

- Volatility surfaces based on (local) stochastic volatility models

- Volatility surfaces based on Levy process

- Volatility surfaces based on models that explicitly specify the dynamics of implied volatility

- Volatility surfaces based on parametric representations

- Volatility surfaces based on nonparametric representations

The thesis describes the basic features of each of these modelling techniques as well as some of the most popular models used by the earlier studies.

Chapter 3 presents the key contribution of this thesis by first introducing various parametric regression models that have been proposed in the prior studies as well as the benchmark models that are used for comparison. In addition, several alternative specifications of the models are also discussed. The next section discusses the use of relatively new concept, namely, promptness, instead of time to maturity, as a factor in the parametric model. Data selection, as an important aspect of a fitting process, is presented in detail. The methodology implemented for surface fitting, including both the equal-weighted scheme, as well as the scheme weighted by observed implied volatilities, are discussed next. Finally, the estimated coefficients and the adjusted R^2 and RMSE statistics of the fits of the models are presented for both the periods with high VIX index levels and low VIX index levels as an indicator for the general level of "stress" in the equity markets and using each fitting scheme.

Chapter 4 presents the summary of the results of the thesis and suggests several further direction of research and improvement that could be made to the models studied in this thesis.

ACKNOWLEDGMENTS

Chapter 1

Background Information

1.1 Introduction to options

Options are financial derivatives where the owners have the right, but not the obligation, to buy or sell underlyings at fixed prices (strike prices) at some points of time in future (the expiration times or the times to maturity). When the owner or buyer of the option has the right to buy at a fixed price, the option is called a call option and when the owner of the option has the right to sell the underlying at a fixed price, the option is called the put option.

During the earlier days of the options trading, there were primarily two types of the options classified by their time of exercise: European and American options. European options can be exercised only at expiration whereas American options could be exercised at any time before expiration. As the market grows and investors demand more flexibility with the options, other exotic derivatives evolve. Few examples are:

- Bermudan Options − The owners have the rights but not the obligation to exercise the options at a set of pre-determined time before the expiration date.

- Asian Options − Instead of the price at the time of exercise, the final payoff is determined by the average of the underlying over a certain period of time.

For options such as Asian options, because the prices of the options are dependent not only on the prices at the expiration dates, but also on the prices of the underlyings during a certain period of time (i.e., the paths of the price of the underlyings), those options are also called path-dependent options. The payoff of the call options is determined by the following formula:

$$\max(X - K, 0)$$

where X is the price of the underlying at the expiration date, if the option is European or the arithmetic average of the price during a certain time in the period specified if the option is Asian. K is the strike price of the option, which in most cases is agreed upon time when the option contract was written (There are also floating strike options, but the discussion of this type of option contract is beyond the scope of this thesis).

Similarly, the payoff of the put option is given by

$$\max(K - X, 0)$$

However, the options have to be priced at the time when they are sold and the spot prices of the underlying at the time of expiration were not known at that time. Hence, the prices of the options, among other things, have to be based on the prices of the underlying at the time of pricing as well as the strike price.

1.2 Volatility and Black-Scholes framework

Volatility measures the degree to which the price of a financial instrument changes over time. Statistically volatility is often measured as the standard deviation of the prices, σ. Based on the ways volatilities are calculated, there are two types of volatility series: historical volatility series and implied volatility series. Historical volatility series is obtained from the historical prices of the financial instruments. Implied volatility, as the name suggests, is the volatility "implied" by the market prices of the derivatives on a financial instrument. As such, in derivatives trading, particularly options trading, implied

volatility is an integral component. In fact, in the options trading world, often implied volatility is quoted instead of price, which is similar to the way yield, instead of actual price, is quoted in the fixed income trading. Accurate modelling of volatility, therefore, is important for the pricing of path-dependent options mentioned above since the volatility throughout the lifetime of the option, not just at expiration, would impact the pricing of the option materially.

Therefore, the conversion between prices and the implied volatility is a topic of interest to many researchers in finance. Fisher Black and Myron Scholes have proposed in 1973 the well-known Black-Scholes model [3], where the derivation is based on the following simplifying assumptions:

1. The market is frictionless and all participants at the markets are able to borrow and lend at a risk-free interest rate.

2. There is no transaction cost.

3. There is no arbitrage in the market.

4. The underlying can be bought in any amount, including fractional units.

5. Finally and most importantly, the underlying follows a geometric Brownian motion with constant drift and constant volatility.

Most of these assumptions are close to reality, especially for large financial institutions. For example, in reality, many financial institutions receive funding rate close to the T-bill rate, which is often used to approximate the risk-free interest rates and, in addition, recent advancement in algorithmic trading and direct market access (DMA) has also made the transaction cost negligible.

1.3   Local volatility and stochastic volatility

Although the Black-Scholes model has several appealing features, such as the existence of close-form solutions that could be computed relatively easily, one of the most unrealistic

assumptions underlying the model, particularly after the financial market crash after 1987, is the time-invariant volatility assumption. As researchers have discovered even before the financial market crash, for equity options that are traded deep in- and out-of-money (i.e., the differences between the strike price and the spot price is large), the options often exhibits much larger volatilities compared to the at-the-money options (i.e., option whose strike and spot prices are the same) or options with strike prices relatively close to the spot prices.

As such, a question arises as to how one could model the volatility of an equity option more accurately? Even for the most liquid exchange-traded equity options, the quoted price is only available at certain strikes for certain pre-defined maturities. As such, only discrete points on the volatility surface could be observed and the remaining unobserved volatilities will have to be derived in order to construct the entire volatility surface.

One naïve approach for generating the volatility is through a simple interpolation, such as a linear interpolation, between the observed volatilities. However, this approach has several critical drawbacks. First, the very assumption that the volatility varies in a linear manner between two different volatilities points is counter-factual. As indicated in Figure 1.1, which is plotted using the experimental data that will be discussed further in the later chapters, we can clearly see a non-linear pattern emerging from the observed volatility points.

Implied Volatility Surface on February 14, 2013
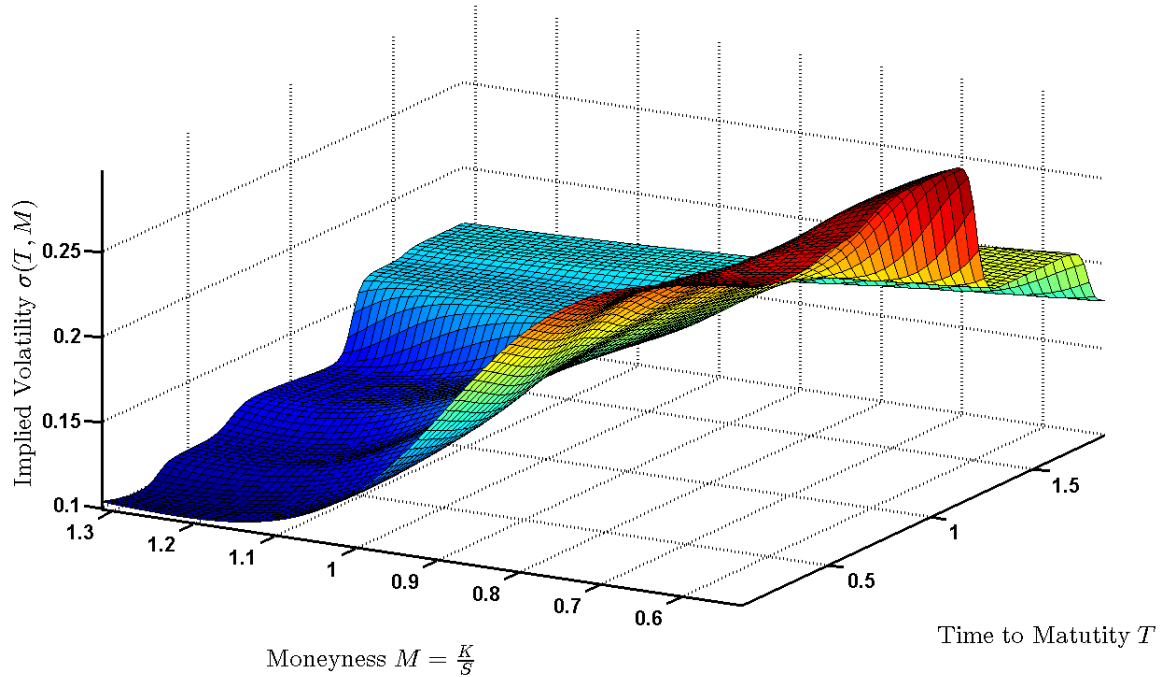
Figure 1.1: Implied Volatility of S&P500 Options on Feb 14, 2013

The term "volatility smile" was first coined by Derman and Kani [11] in 1994. It was proposed that instead of assuming volatility to be deterministic, the volatility of options could be modelled better by assuming that it is a function of both the spot price and the time to maturity. Using this definition, the volatility is only held constant "locally" to the specific underlying price level and the specific time to maturity. The term local volatility has since surfaced prominently in the finance literature. We can see from the graph above, there are many sections of the graph that are relatively "flat", hence if the changes in spot price level (δs) and time to maturity (δt) are small, the volatility surface could be approximated to a constant.

However, in Derman-Kani's model, the stock price (and, hence, the implied volatility) is modelled as a tree, which means that the price is modelled as a discrete-time random process, whereas modelling the stock process using a continuous-time process would fits the reality better.

5

Dupire [13] showed that provided certain conditions are met, it is possible to have the local volatility specified in a continuous-time framework:

$$\frac{\partial C}{\partial T} = \frac{1}{2}\sigma^2(K, T; S_0)K^2\frac{\partial^2 C}{\partial K^2} - (r - D)K\frac{\partial C}{\partial K} - DC$$

where:

- C = short form of $C(S_0, K, T)$, which is the price of a call option with time to maturity T and strike price K,

- D = short form of $D(T)$, which is the instantaneous dividend rate,

- r = short form of $r(T)$, which is instantaneous risk-free rate,

- σ = implied volatility, which is defined as a function of K, T and S_0,

- S_0 = price of the underlying security at time 0,

- K = strike price of the option.

Stochastic volatility models assume that the volatility of underlying securities follows a stochastic process. The general form of the stochastic volatility model can be specified as:

$$dS_t = \mu S_t dt + \sqrt{\nu_t}S_t dW_t^1$$
$$d\nu_t = \alpha_{\nu_t,t}dt + \beta_{\nu_t,t}dW_t^2$$

where:

- μ = constant drift factor of the price process of the underlying,

- ν_t = volatility factor of the price process of the underlying,

- S_t = price of the underlying at time t,

- W_t^1, W_t^2 = Wiener processes, assumed to be correlated with a constant coefficient of correlation ρ.

- $\alpha_{\nu_t,t}, \beta_{\nu_t,t}$ = random processes which depends on ν_t and t.

A particular specification of this model is given by Heston [17] in 1993.

Heston's Stochastic Volatility Model [17] is one of the most widely used stochastic volatility models today due to the existence of closed-form solutions for pricing purposes. In essence, the instantaneous variance of Heston's model is a square-root process model described by Cox, Ingersoll and Ross [9]. Heston's model can be written as:

$$dS_t = \mu S_t dt + \sqrt{\nu_t} S_t dW_t^1$$
$$d\nu_t = \theta(\omega - \nu_t)dt + \xi\sqrt{\nu_t}dW_t^2$$

where μ, ν, W_t^1 and W_t^2 are defined as above and,

- θ = rate of mean reversion for ν.

- ω = mean reverting factor.

- ξ = volatility of volatility.

Note that in this model, the price process of the underlying is not a mean-reverting process; however the volatility process does exhibit mean-reversion. Such an assumption is consistent with the empirical evidence suggested by Gatheral [15]:

- The daily return and daily log return distributions tend to show fat tails and high central peak, which is a sign that the return distribution is a mixture of distributions with different variances,

- The "volatility-clustering" feature, i.e., period with rapid moves in return is often followed by periods with rapid moves and period with small moves is often followed by such as well, which seems to indicate that the variance process is a mean-reverting process.

Chapter 2

Recent Development of Volatility Modelling

2.1   Introduction

Even though it has been almost two decades since the idea of local volatility was first proposed, it continues to be an active research area in finance. Over the years, several new models have been proposed in order to more accurately capture the volatility surface without sacrificing too much on the speed and efficiency of the computation to make it impractical, given the limited and discrete observable data sets.

Homescu [18] has summarized them into the following categories:

- Volatility surfaces based on (local) stochastic volatility models.

- Volatility surfaces based on Lévy process.

- Volatility surfaces based on models that explicitly specify the dynamics of implied volatility.

- Volatility surfaces based on parametric representations.

- Volatility surfaces based on nonparametric representations.

2.2 Volatility surfaces based on (local) stochastic volatility models

Various(local) stochastic volatility models are proposed to model the volatility surfaces. Other than the Heston's model mentioned above and some of its extensions, which is based on the Cox-Ingersoll-Ross (CIR) process, there is also the Stochastic Alpha, Beta, Rho (SABR) stochastic volatility model proposed by Hagan, *et. al.* [16]. SABR Stochastic Volatility Model is based on the Constant Elasticity of Variance (CEV) model, which was proposed by Cox [8] in 1975.

The dynamics of the CEV model is:

$$dS_t = \mu S_t dt + \sigma S_t^\gamma dW_t$$

where $\sigma \geq 0$, $\gamma \geq 0$, and the dynamics of the SABR Stochastic Volatility Model is:

$$dF_t = \sigma_t F_t^\beta \ dW_t$$

$$d\sigma_t = \alpha \sigma_t \ dZ_t$$

$$d\langle W_t, Z_t \rangle = \rho dt$$

where $0 \leq \beta \leq 1$, $\alpha \geq 0$, F_t is the price of the underlying and ρ is the correlation between the two Geometrical Brownian Motion (GBM), W_t and Z_t.

The local-stochastic volatility (LSV) models are mixtures of the stochastic and local volatility models designed with those features observed from both stochastic and local volatility models. It often uses one of the stochastic volatility models such as the Heston's model as the base model but with the local volatility component (σ_{LSV}(S(t),t)) to model the price process. This is different from the Heston's model in which the stochastic component of the price process depends, other than the volatility process itself, only on

the price of the underlying, S_t. Using the previous notation we have used to describe the Heston's model, an example of the LSV model could be:

$$dS_t = \mu S_t dt + \sigma_{LSV}(S(t), t)\sqrt{\nu_t} S_t dW_t^1$$
$$d\nu_t = \theta(\omega - \nu_t)dt + \xi\sqrt{\nu_t}dW_t^2$$

where $\sigma_{LSV}(S(t), t)$ is the local volatility component of the process, other symbols such as ν_t and ξ are defined the same way as the Heston's Model.

Among the different stochastic volatility models, Heston's model continues to be one of the most commonly-used models due to the existence of analytical solutions, with several extensions proposed in order to enhance the ability of the model to produce the dynamics that are consistent with those seen in the real market.

2.3   Volatility surfaces based on Lévy

process Lévy processes have a jump component added to the price processes of the underlying. By incorporating the jump component in a diffusion process, short-term skews can be modelled better compared to a pure diffusion process. One of the most popular models in this family is Variance Gamma model proposed by Madan and Seneta in 1990 [23] and popularized by Madan, Carr and Chang in 1998 [24] . The Variance Gamma (VG) process is can be constructed by first adding a drift component that follows the gamma process to the standard Brownian motion, making it a shifted Brownian Motion, i.e.,

$$b(t; \theta, \sigma) = \theta t + \sigma W(t)$$

where $W(t)$ is a standard Brownian motion.

Now if we make the time in the Brownian motion to stochastic and follows with unit mean rate, i.e., $t \sim \gamma(t; 1, \nu)$, then we can define a VG process

$$X(t)$$

as:

$$X^{VG}(t; \sigma, \nu, \theta) := b(\Gamma(t; 1, \nu); \theta, \sigma)$$

where

σ = volatility of the Brownian motion,

ν = variance rate of the gamma time change,

θ = drift in the Brownian motion with drift.

Then, under the risk neutral measure, the price process can be defined by:

$$S(t) = S(0)exp(rt + X^{VG}(t; \sigma, \nu, \theta) + \omega t)$$

with

$$\omega = \frac{1}{\nu} \log(1 - \theta\nu - \frac{1}{2}\sigma^2\nu).$$

By assuming that the stock price follows a variance gamma process instead of lognormal process, it allows better modelling of higher moments and thus consistent derivatives pricing using a single set of parameters instead of modelling using a parameter set specific to a strike level and/or time to maturity.

2.4 Volatility surfaces based on models for the dynamics of implied volatility

Instead of assuming that the dynamics of the models would fit into the observed implied volatility, another approach specifies the dynamics of the observed implied volatility directly. Such models are called the "market models". One such example is proposed by Ledoit and Santa-Clara in 1998 [22], which shows that the stochastic volatility is equal to the implied volatility of at-the-money call options when the time to maturity is approaching zero. The joint process could then be derived by the no-arbitrage principles.

The problem with such an approach is that we cannot choose any martingale component of the dynamics, as pointed out by Carr and Wu [4] in 2012. They have proposed an alternative approach which models the future risk-neutral dynamics of the implied volatility across different strikes and expiration dates instead of modelling the instantaneous variance rate. The no-arbitrage constraints are then derived for the implied volatility surface. This is argued to result in an improvement to the Heston's model. For example, the log-normal implied variance dynamics (LNV) is shown to have the following four advantages compared to the Heston's model by Carr and Wu [4]:

- Half of the root-mean-squared error,

- Explained 4% more variation,

- Generated errors with lower serial correlation,

- 100 times faster in calibration.

2.5 Volatility surfaces based on parametric representations

Parametric representation approach uses various regression models in a parametric specification, which is computationally much less expensive compared to the calibration of the Heston's model and its extensions.

The first type of parametrization used to generate volatility surfaces is based on a polynomial function, which will be discussed in more details in the next chapter. Another approach was proposed by Gatheral [14] in 2004. In this approach, he termed such a model Stochastic Volatility Inspired (SVI) parametrization.

Let $S_0 :=$ spot price of the underlying security and K := strike price of the option, Then, $k = \log \frac{S_0}{K}$.

The SVI parametrization can be specified as:

$$\sigma_{SVI}^2 = a + b\{\rho(k - m) + \sqrt{(k - m)^2 + \sigma^2}\}$$

where:

σ_{SVI}^2 = SVI parametrization of the total implied variance

a = overall level of variance,

b = angle between left and right asymptotes,

σ = smoothness of the vertex,

ρ = orientation of the graph,

m = translation of graph.

- left asymptote: $\sigma_L^2(k; a, b, \sigma, \rho, m) = a - b(1 - \rho)(k - m)$, and

- right asymptote: $\sigma_R^2(k; a, b, \sigma, \rho, m) = a + b(1 - \rho)(k - m)$.

The model parameters are calibrated by minimizing the sum of squared differences between the SVI and the Black-Scholes implied volatility, namely:

$$min(\sum_{i=1}^{n}(\sigma_{SVI}^i - \sigma_{BS}^i)^2).$$

where:

- σ_{SVI}^i is the implied volatility using SVI parametrization, based on the ith observation,

- σ_{BS}^i is the implied volatility under Black-Scholes framework, based on the ith observation.

Gatheral proved that the SVI is consistent with implied variance skew shown in the Heston's model.

2.6 Volatility surfaces based on nonparametric representations

By using nonparametric representations, we no longer need to be concerned with fitting the implied volatility surface to a particular functional form. Instead, the effort is focused on the interpolation techniques to ensure the surface is arbitrage-free. One such algorithm was proposed by Kahale [21] in 2004, which assumed that the observed implied volatility surface follows no-arbitrage principle. For each dimension, the arbitrage-free interpolation is computed for options with different maturities. For each maturity, the corresponding squared implied volatility of the same strike is interpolated linearly. Further adjustment was made to ensure that the entire surface is arbitrage-free.

There are also several other approaches, such as spline interpolation using regular cubic splines, cubic B-splines and thin splines, as well as discretization based on Dupire forward PDE, which were elaborated in more detail in Homescu [18].

Chapter 3

Parametric Representation and Its Extensions

3.1 Introduction

We begin our discussion in this chapter by first introducing some notations:

Let V_t be the price of a European style option with strike price K,

S_t be the price of the underlying security at time t,

$\tau_t := T - t$ where T is the maturity time, hence τ_t is the time to maturity of the option at time t for option expiring at time T, to simplify the notation, we will use τ in place of τ_t in the remainder of this thesis,

$r_t :=$ risk-free interest rate at time t,

$\sigma_t(V_t, \tau) :=$ implied volatility of the option with value V_t and time to maturity τ, i.e. it satisfies the following Black-Scholes equation,

$$V_t(\tau) = \begin{cases} N(d_1)S_0 - N(d_2)Ke^{-r(\tau)}, & \text{if the option is a call option.} \\ N(-d_2)Ke^{-r(\tau)} - N(-d_1)S_0, & \text{if the option is a put option.} \end{cases} \tag{3.1}$$

$$d_1 = \frac{1}{\sigma\sqrt{\tau}}\left[\ln\left(\frac{S_t}{K}\right) + \left(r_t + \frac{\sigma^2}{2}\right)(\tau)\right]$$

$$d_2 = \frac{1}{\sigma\sqrt{\tau}}\left[\ln\left(\frac{S_t}{K}\right) + \left(r_t - \frac{\sigma^2}{2}\right)(\tau)\right]$$

$$= d_1 - \sigma\sqrt{T-t}$$

Regression approach was first suggested by Dumas *et. al.* [12]. In this approach, the implied volatility is expressed as a function of the strike price K and time to maturity T. Four models have been proposed:

- **Model 0:** $\sigma_t(V_t, \tau) = \alpha_0$

- **Model 1:** $\sigma_t(V_t, \tau) = \alpha_{0,t} + \alpha_{1,t}K + \alpha_{2,t}K^2$

- **Model 2:** $\sigma_t(V_t, \tau) = \alpha_{0,t} + \alpha_{1,t}K + \alpha_{2,t}K^2 + \alpha_{3,t}\tau + \alpha_{4,t}K\tau$

- **Model 3:** $\sigma_t(V_t, \tau) = \alpha_{0,t} + \alpha_{1,t}K + \alpha_{2,t}K^2 + \alpha_{3,t}\tau + \alpha_{4,t}\tau^2 + \alpha_{5,t}K\tau$

Model 0 is consistent with the Black-Scholes model with constant volatility.

Cont and Fonseca [7] suggested that the implied volatility could be modelled better as a function of time to maturity τ and moneyness m_t, where:

$$m_t = K/S_t$$

where K is the strike of option and S_t is the price of the underlying at time t, also known as the spot price. Following this argument, Alentorn [1] improved the models by making implied volatility explicitly a function of moneyness and time to expiration.

The following notations are used in Alentorn's models:

Modified moneyness, $\hat{M}_t$, is defined as

$$\hat{M}_t = (\log(F_t/K))/\sqrt{\tau}$$

F_t is the implied forward price of the underlying at time t, which can be expressed as:

$$F_t = S_t \exp\left(r_t t\right)$$

The models proposed by Alentorn [1] can be recast in regression framework as follows:

- **Model 0:** $\sigma_t(\hat{M}_t, \tau) = \beta_{0,t} + \epsilon_t$

- **Model 1:** $\sigma_t(\hat{M}_t, \tau) = \beta_{0,t} + \beta_{1,t}\hat{M}_t + \beta_{2,t}\hat{M}_t^2 + \epsilon_t$

- **Model 2:** $\sigma_t(\hat{M}_t, \tau) = \beta_{0,t} + \beta_{1,t}\hat{M}_t + \beta_{2,t}\hat{M}_t^2 + \beta_{3,t}\tau + \beta_{4,t}\tau\hat{M}_t + \epsilon_t$

where ϵ_t is assumed to be identically and independently distributed with mean 0 and constant and finite variance.

Badshah [2] provides a fourth extension to include the T_t^2 term as an additional explanatory variable in the regression:

Model 4: $\sigma_t(\hat{M}_t, \tau) = \beta_{0,t} + \beta_{1,t}\hat{M}_t + \beta_{2,t}\hat{M}_t^2 + \beta_{3,t}\tau + \beta_{4,t}\tau\hat{M}_t + \beta_{5,t}\tau^2 + \epsilon_t$

The last explanatory variable, τ^2 was added to capture the curvature of the implied volatility surface along the time-to-maturity axis.

Subsequently, Roux [25] proposes another model which takes into account of VIX index, the volatility index of S&P 500, and a modified version of maturity and moneyness, as:

Model 5: $\sigma_t(\hat{m}_t, \tau) - VIX_t = \alpha_{0,t} + \alpha_{1,t}\log\hat{m}_t + \alpha_{2,t}\frac{1}{\sqrt{\tau}} + \alpha_{3,t}(\log\hat{m}_t)^2 + \alpha_{4,t}\frac{\log\hat{m}_t}{\sqrt{\tau}} + \alpha_{5,t}\frac{(\log\hat{m}_t)^2}{\sqrt{\tau}} + \epsilon_t$

where VIX_t is the spot VIX index at time t. The VIX index measures the 30-day expected volatility of the S&P 500 index [5]; in other words, it is a measurement of short-term volatility. However, our analysis will show that by removing VIX from the implied volatility data, the remainder could be well-explained by the regression models, during both the stressed and non-stressed periods. The stressed and non-stressed periods are measured by the magnitude of VIX index itself which will be explained in detail in the later sections of this chapter.

The model proposed by Roux has six different parameters at each time step t. Roux deploys Principal Component Analysis (PCA) techniques to reduce the dimension of the model.

PCA is a technique used to reduce the dimensionality of a dataset consisting of a large number of interrelated variables, while retaining as much as possible of the variation present in the dataset[20]. The resulting set is called Principal Components (PCs), which are orthogonal to each other.

Roux suggests that the variation in volatility surface can be explained by the VIX index and one or two other uncorrelated factors, i.e.,

$$\sigma_t \approx \alpha_0 + VIX_t\alpha_1 + k_{1,t}b_1 + k_{2,t}b_2$$

where b_1 and b_2 are the two principal components other than VIX. The principal components are orthogonal to VIX index, and the principal components b_1 and b_2 are orthogonal to each other.

Furthermore, Roux also argues that $k_{1,t}$ and $k_{2,t}$, the time-dependent coefficients, are not independent of each other. In fact, Roux discovers that the correlation between $k_{1,t}$ and $k_{1,t-1}$ is 91.0% and that of $k_{2,t}$ and $k_{2,t-1}$ is 84.6% based on his data. As such, they can be modelled to follow a first-order autoregressive process:

$$k_{i,t} = \beta_i k_{i,t-1} + \gamma_i \epsilon_{i,t}$$

where the error term $\epsilon_{i,t}$ is assumed to be a white-noise process.

In order to test the effectiveness of the regression models, benchmark models have been proposed. The so-called Practitioner Black-Scholes (PBS) model is very similar to Model 4. It is originally proposed by Dumas *et. al.* [12] and stated as:

PBS: $\sigma_{K,\tau}(\theta) = \theta_{0,t} + \theta_{1,t}K + \theta_{2,t}K^2 + \theta_{3,t}\tau + \theta_{4,t}\tau^2 + \theta_{5,t}K\tau + \epsilon_t$

In this version of the PBS, the volatility surface is independent of the price of the underlying. Rather, it is dependent on the strike price of the option. As such this is the

same model as the one used to describe the evolution of volatility smile which is coined by Derman [10], a "sticky-strike" rule.

Another version of the model is proposed by Christoffersen and Jacobs [6], which, instead of using a function of K, uses a function of moneyness. This is defined as S/K (i.e., the ratio of spot price to strike price, which is the reciprocal of the moneyness that was defined in the previous models) and the rest of the specification is similar to the previous version of PBS model:

PBS: $\sigma_{S_t/K,\tau}(\theta) = \theta_{0,t} + \theta_{1,t}(S_t/K) + \theta_{2,t}(S_t/K)K^2 + \theta_{3,t}\tau + \theta_{4,t}\tau^2 + \theta_{5,t}(S_t/K)\tau + \epsilon_t$

In this version of the PBS, the volatility surface is independent on moneyness, instead of strike in the previous version of PBS. Therefore, this form of implied volatility is named a "sticky-moneyness" rule.

Based on the models presented above, we propose further candidate models in an attempt to better fit the observed implied volatility surface, and test the resulting fitting models against various stressed and non-stressed periods.

The contribution of this chapter is three fold:

1. We propose several variations of Roux's models for periods characterized by unusually high and low market volatility as proxied by the VIX index, since we have observed from historical data that merely modelling using the quadratic terms of log moneyness and the square-root terms of the time to maturity may not adequately explain the shape of the volatility surface over the sample period, which is admittedly unrepresentative as it includes episodes of unusually high and low market volatility before, during and after the global financial crisis.

2. We discriminate various regression specifications during both the stressed and non-stressed periods, as determined by the VIX index, and confirm that the proposed models provide good fits regardless of the period used for estimation.

3. Furthermore, we also explore an alternative factor of using promptness in place of time to maturity as an option.

The rest of the chapter is organized as follows:

- In Section 3.2 we discuss several potential issues concerning the models proposed by Roux [25] and propose new specifications with additional explanatory variables which we hope to lead to improvement of the fit of the models and thus, better construction of the implied volatility surface,

- in Section 3.3, we discuss the use of promptness, instead of the more commonly used absolute time to maturity, to the regression models. In doing so, we hope to make the model more transient at an affordable loss of accuracy,

- in Section 3.4, we discuss the data that we are using for our empirical analysis, including the source and the relevant data cleaning we have to do,

- in Section 3.5, we discuss the methodology used to fit the implied volatility surface,

- in the final section of this chapter, we discussed the relevant result and our empirical findings.

3.2   Variations of Roux's model

The model proposed by Roux [25] is based on several empirical observations from a particular sample period. One of the key observations is that, in general, VIX index moves in line with the trailing implied volatility of S&P 500 index, which is measured as an exponential moving average of the index weekly returns, but VIX is usually higher.

Note that if the Black-Scholes model actually holds, we should expect the implied volatility of S&P 500 options to match exactly to the trailing S&P 500 volatility, i.e.,

$$\sigma_t(\hat{M}_t, \tau) - \text{VIX} = 0 \ \ for \ \ any \ \ \hat{M}_t \ \text{and} \ \tau. \tag{3.2}$$

However, this is not consistent with the empirical evidence for our sample period. In fact, as illustrated in Figure 3.1, the trailing volatility of the index can differ quite significantly from the actual VIX index.
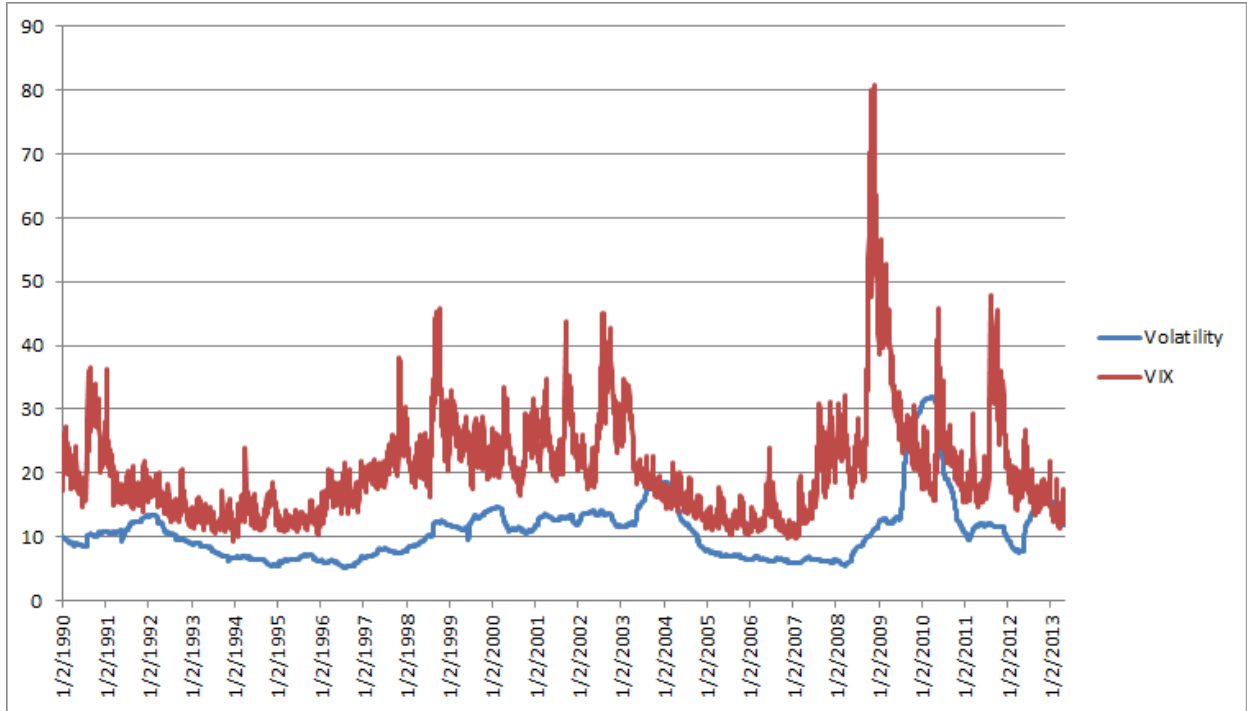
Figure 3.1: **S**&P500 Historical Volatility Versus VIX Index

This is yet another piece of evidence that the standard Black-Scholes model alone with constant volatility may not be adequate in explaining the volatility surface of S&P500 options.

The explanatory variables in Roux's model are also determined by the observed shape of the graphs when plotting the implied volatility against the response variables. The two main observations outlined by Roux [25] are:

- When implied volatility is plotted as a function of simple moneyness, m, and time to maturity, τ, which defined by

$$M = \frac{-r\tau - \log m}{\sqrt{\tau}},$$

the resulting graph is roughly parabolic in shape,

- for a given level of moneyness, the implied volatility appears to be a linear function of the square root of time to maturity, $\sqrt{\tau}$.

21

In order to verify whether the observations claimed above continue to hold true for our sample period which includes episodes before, during, and after the global financial crisis, several graphs have been plotted in Figure 3.2:
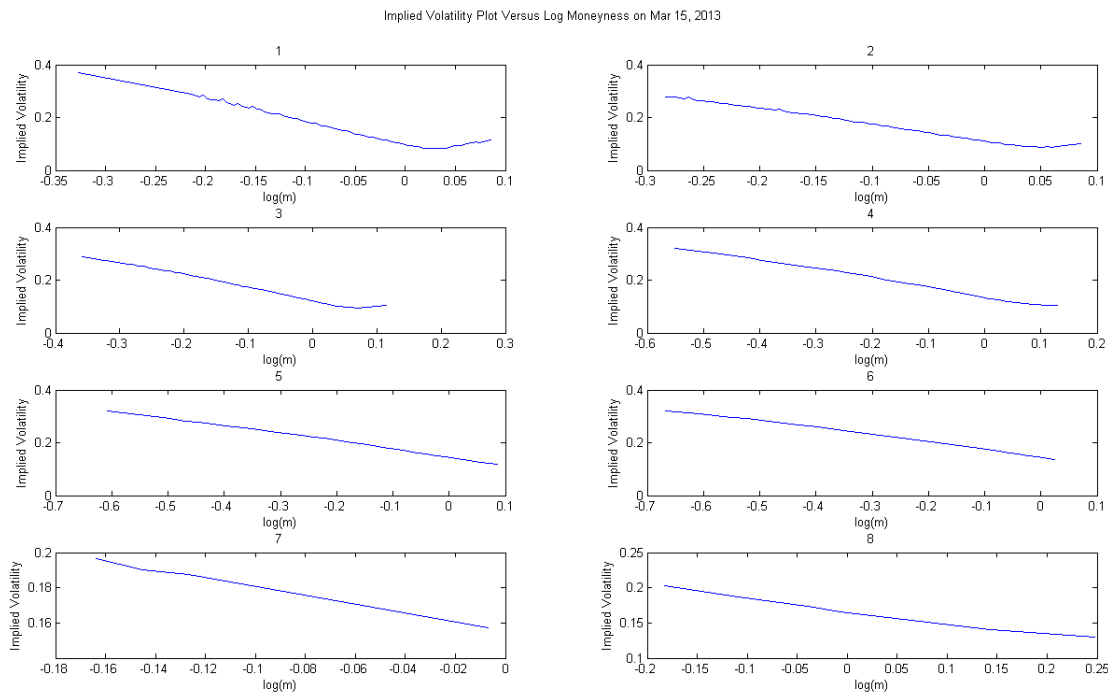

Figure 3.2: Implied Volatility Versus Log Moneyness on March 15, 2013

The graph shows the implied volatility versus log moneyness on March 15, 2013, which is one of the periods with relatively low VIX index levels. The number on top of each graph shows the promptness of the option contract, i.e., the first prompt refers to the option contracts that will expire the soonest on that day and the prompt 2 refers to the option contracts that will expire after the first prompt and so on. Further discussions on promptness will be provided later on in this chapter. As seen from the graph, at least for the first four prompt contracts, the implied volatility versus log-moneyness plots seem to resemble relatively closely to a quadratic function in shape.

Another plot is created for February 14, 2013, which is another period with relatively low VIX index and seems to draw the same conclusion, as demonstrated in Figure 3.3:
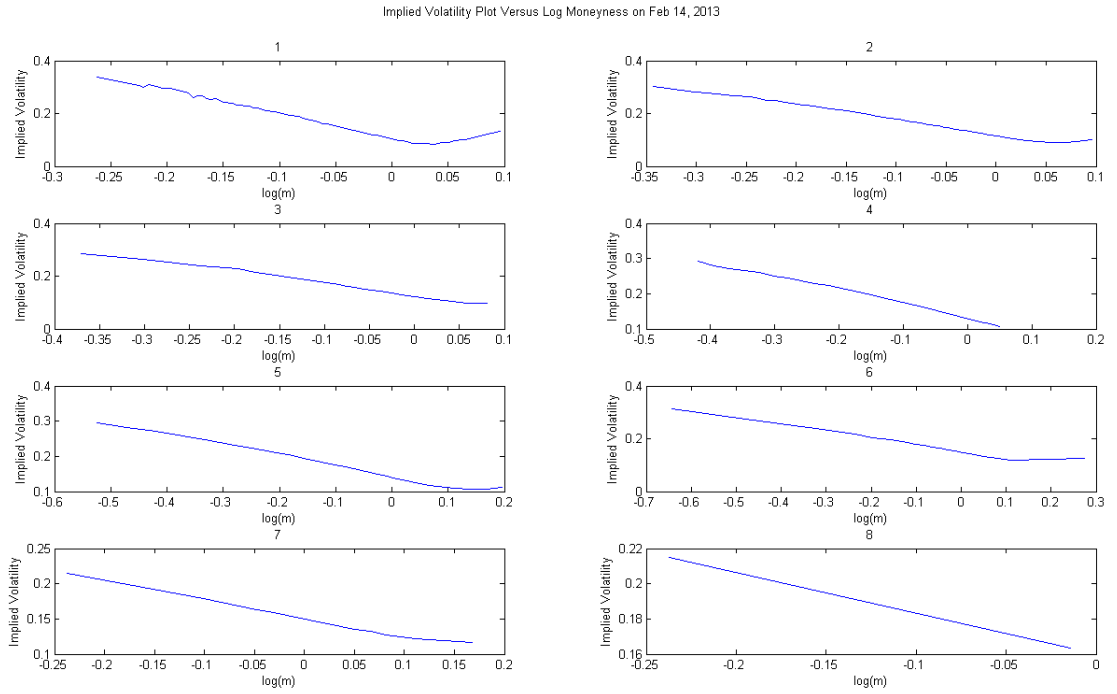
Figure 3.3: Implied Volatility Versus Log Moneyness on February 14, 2013

In fact, in this plot, some of the even longer-dated maturity options are showing a parabolic shape as well.

The plots above show the pattern when the VIX index is relatively low; however during the periods when the VIX index is relatively high, the parabolic shape is no longer so visible. For instance, Figure 3.4 shows the implied volatility versus log-moneyness on May 21, 2010, when VIX index was at a relatively high level of 40.1:
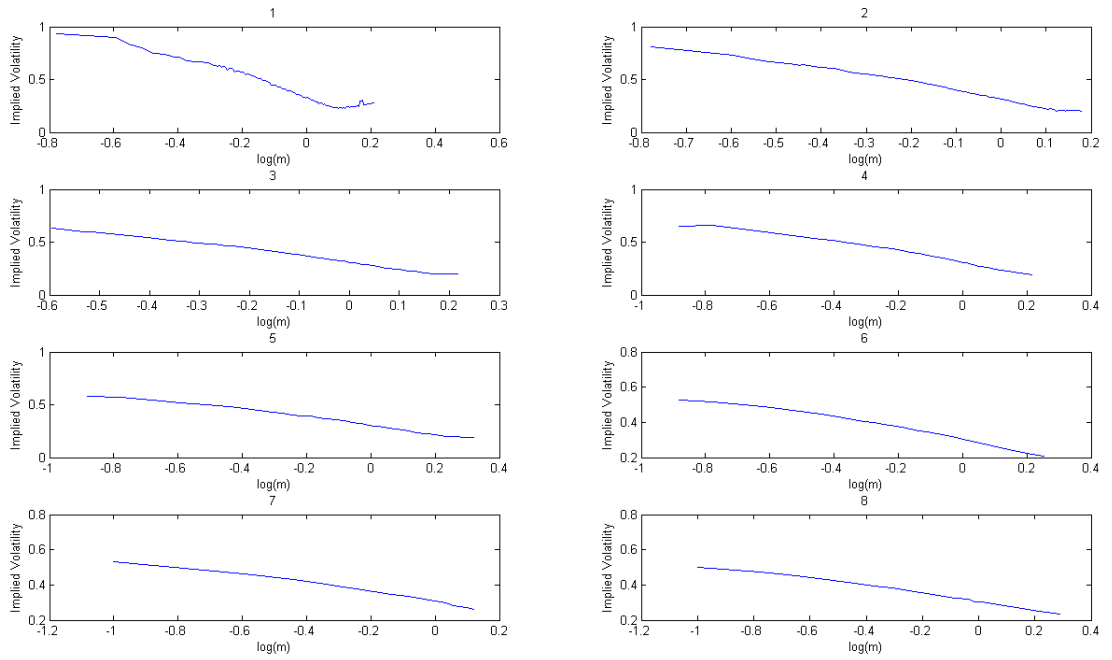
Figure 3.4: Implied Volatility Versus Log Moneyness on May 21, 2010

From the graph, it can be observed that, for the first prompt at least, the plots exhibit shapes that can not be adequately approximated by a quadratic function; instead they seem to require a higher-degree polynomial function.

When the VIX index is at very a high level, such as observed around October 2008, the plotted graph is even less consistent with a quadratic function:
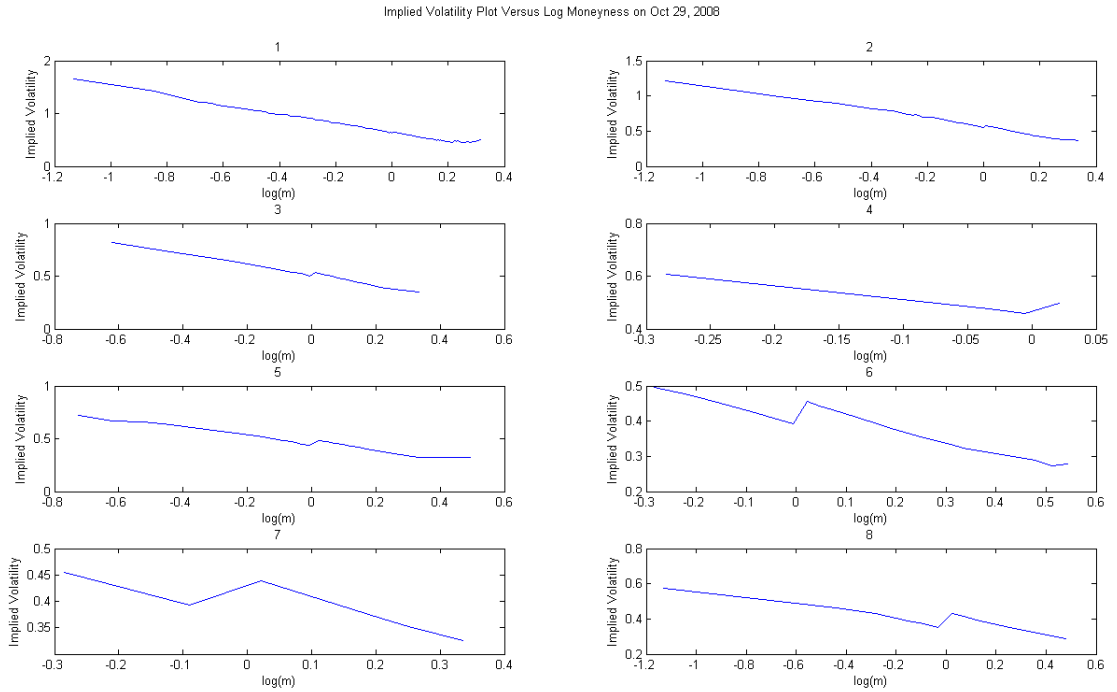
Figure 3.5: Implied Volatility Versus Log Moneyness on October 29, 2008

The above plot shows the implied volatility versus log-moneyness on October 29, 2008, four trading days after VIX index reached its historical high of 81.65 (the highest intra-day level on October 29 was 71.74). "Kinks" on the graph are observed at around at-the-money level (i.e., when $\log(m) = 0$). More importantly, the graph no longer exhibits the shape of a quadratic function.

As such, higher degree polynomials may be necessary to model the implied volatility surface. Such models will be proposed later on in this section.

The second observation is that the implied volatilities for a given strike seem to follow a linear relationship when plotted against $\frac{1}{\sqrt{\tau}}$. In order to verify this claim, the implied volatility versus $\frac{1}{\sqrt{\tau}}$ are plotted for the four dates used in verifying the first claim:
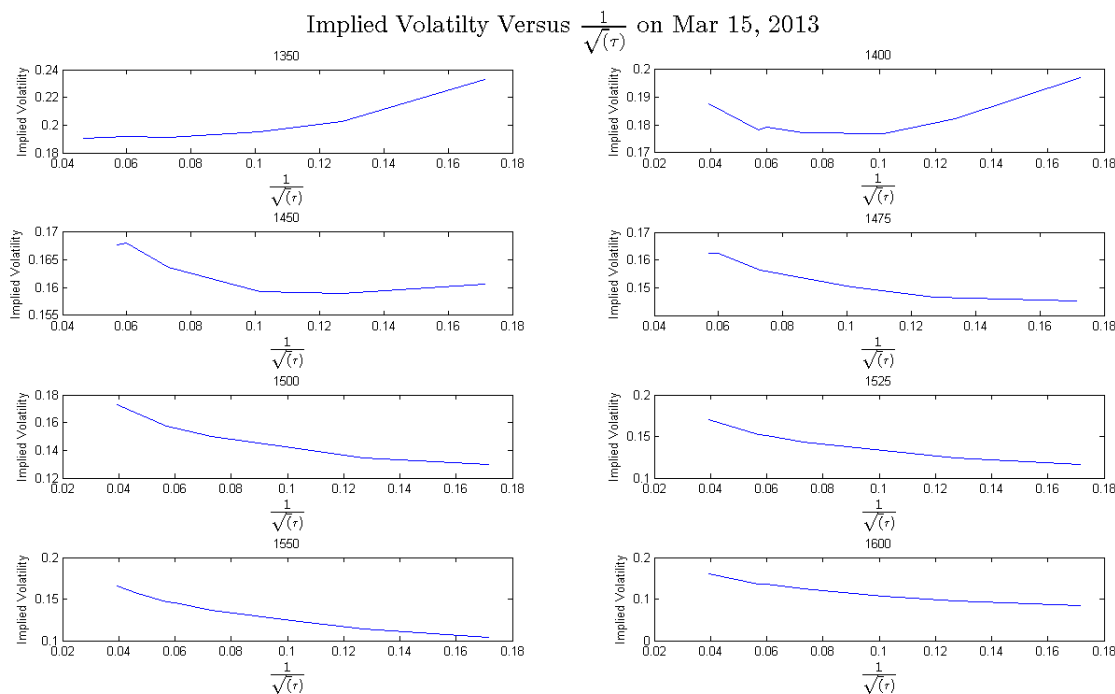
25

Figure 3.6: Implied Volatility Versus $\frac{1}{\sqrt{\tau}}$ on March 15, 2013

Figure 3.6 shows the implied volatility versus $\frac{1}{\sqrt{\tau}}$ on March 15, 2013. As we have mentioned earlier, it is one of the periods with relatively low VIX index levels. The number on top of each subplot indicates the strike price of the options in the plot. Note that the data used is taken from the out-of-money call and put options. As such, since the S&P 500 index was trading between 1555-1563 on that day, this graph shows mostly the out-of-money call options (strike price below spot price, i.e., where strike price are in the range of 1350 to 1550) and one out-of-money put option (strike at 1600). Furthermore, only the graphs of the options with more than five maturity periods being traded (i.e., maturity periods with trading volume greater than 0) are plotted to ensure that there is a sufficient number of data points for analysis. Finally, days, instead of years, are used for time to maturity. From the graph, we can see that none of the plots seems to indicate a linear relationship.

Figure 3.7 uses the data on February 14, 2013, which is the second day with relatively

low VIX index levels:
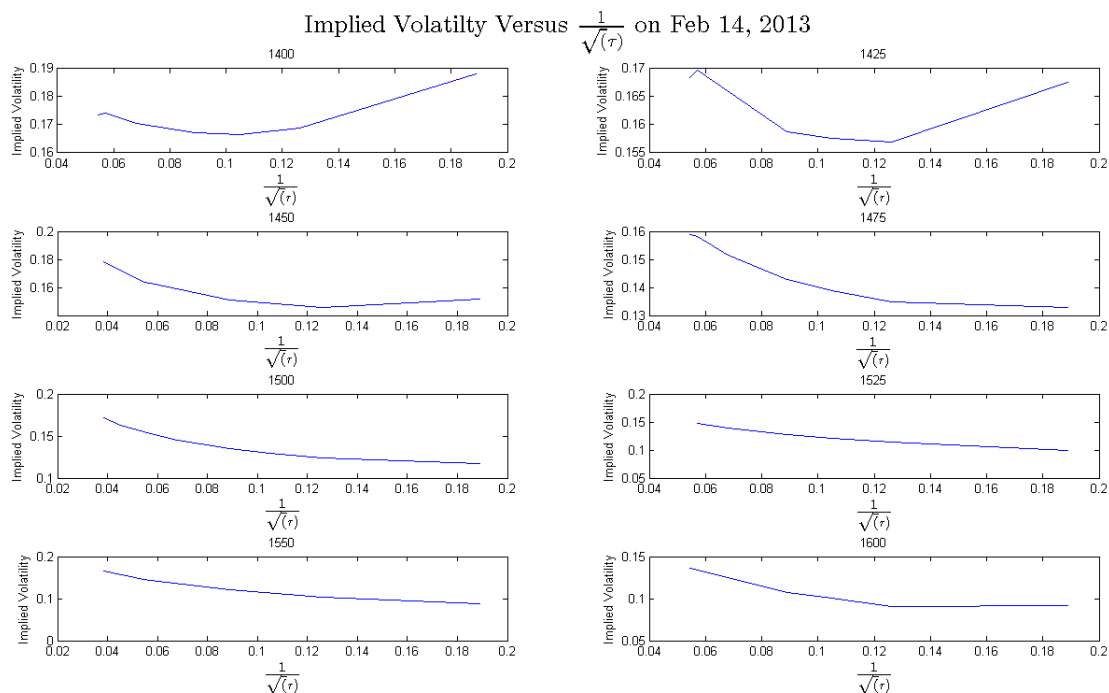
Figure 3.7: Implied Volatility Versus $\frac{1}{\sqrt{\tau}}$ on February 14, 2013

The S&P 500 index was trading at 1514-1523 on that day; hence the plot is showing five out-of-money call options and three out-of-money put options (strike levels 1525, 1550 and 1600). From the graph, it can be seen that except the two close to the at-the-money options (strike level 1525 and 1550), the curves resemble somewhat a linear shape; all of the other plots have clearly shown curvatures that could not be adequately approximated by a linear relationship.

Similar to what was done to verify the first claim, plots for days with relatively high VIX index levels are provided as well. Figure 3.8 shows the implied volatility versus $\frac{1}{\sqrt{\tau}}$ on May 21, 2010, when VIX index was at a relatively high level of 40.1:

27
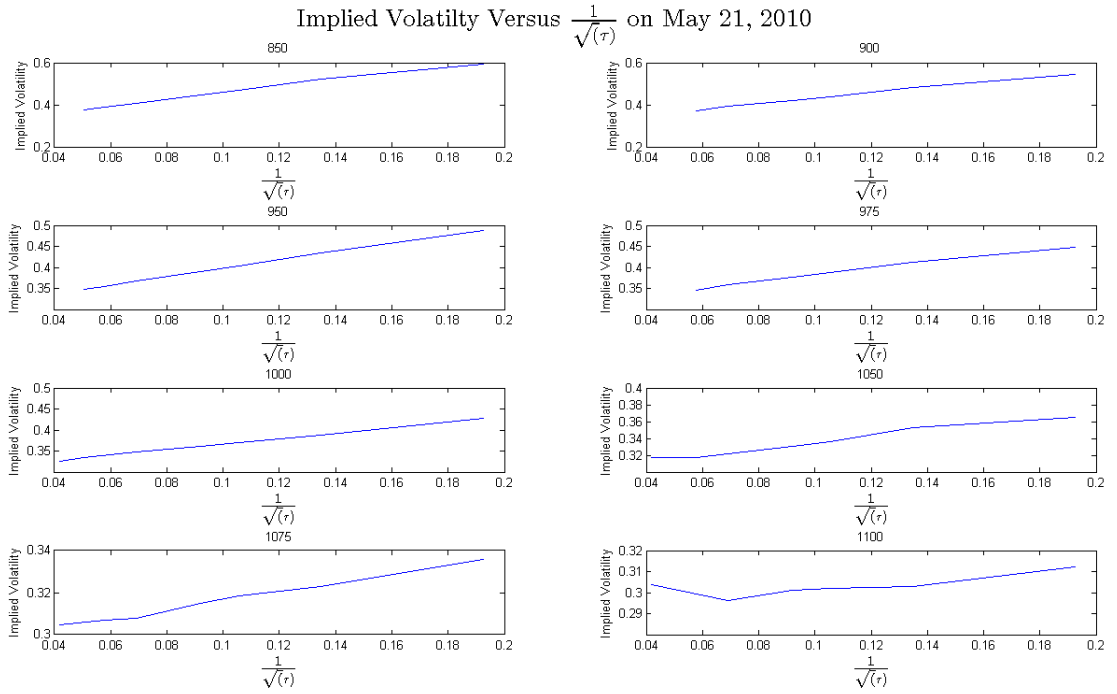
Figure 3.8: Implied Volatility Versus $\frac{1}{\sqrt{\tau}}$ on May 21, 2010

The S&P 500 index was trading in the range of 1055-1090 on that day; hence this plot consists of six out-of-money call options and two out-of-money put options. For the out-of-money call options, surprisingly, the plot seems to show a trend that is closer to a linear relationship. For instance, for strike levels 975 and 1000, the curves appear to be very close to a straight line.

Figure 3.9 shows the data on October 29, 2008, when the VIX was at a very high level:
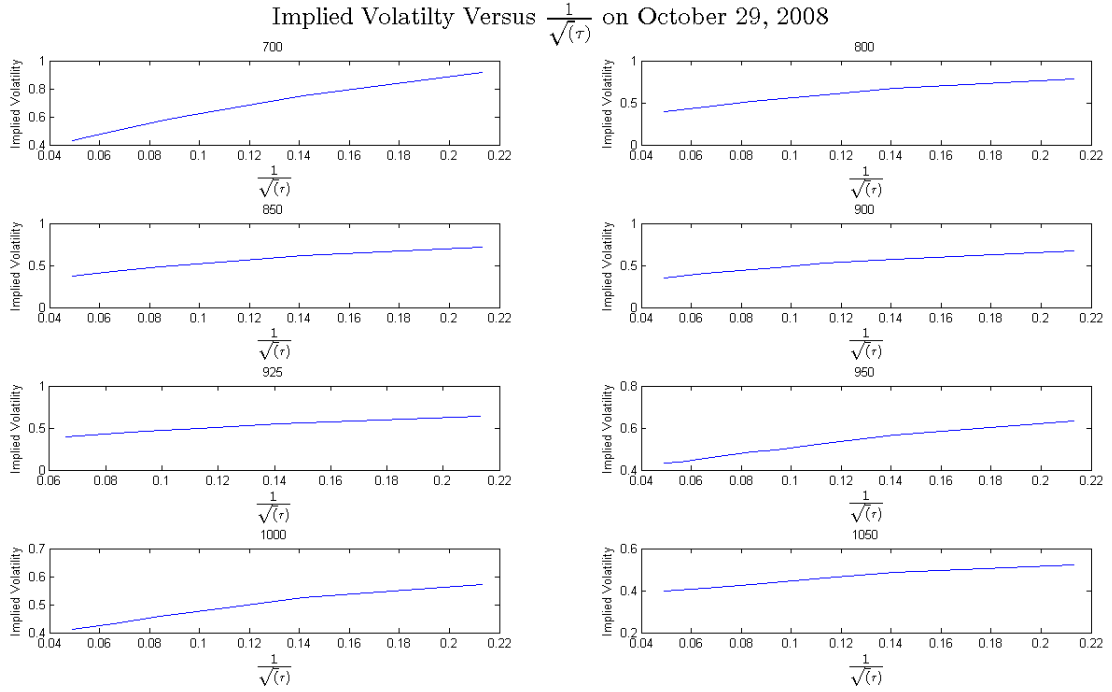
Figure 3.9: Implied Volatility Versus $\frac{1}{\sqrt{\tau}}$ on October 29, 2008

The underlying S&P 500 index was trading at 922-970 levels on that day and for both out-of-money call and put options, linear patterns seem to have emerged from the plots, and this is fairly consistent among all strike levels.

Thus, we can see that during the periods where the VIX index levels are relatively high, the linear pattern appears to be more visible. One possible explanation for this result is that the liquidity of the market tends to be worsened at time of high market volatility, and as a result there is are relatively fewer data points available. Hence the plots could be fitted relatively well in a linear pattern. However, during the time of relatively low VIX index levels, it is obvious that linear relationships are not sufficient to approximate the shapes of the curves.

Furthermore, Roux [25] mentioned a subtle but important limitation of the model; that is, the parabolic shape breaks down when the options are deep out-of-money. Using

29

the put-call parity condition, which states the following [19]:

$$c + Ke^{-rT} = p + s_0$$

where

- $c=$ price of the European call option

- $p=$ price of the European put option

- $K=$ strike price of the European options

- $r=$ risk-free interest rates

- $T=$ time to maturity

- $s_0 =$ spot price of the underlying

We can see that the parabolic shape also breaks down when the options are deep in-the-money, since the volatility of a call option deep in-the-money would be similar to a put option that is deep out-of-money and vice-versa.

In summary, essentially the parabolic shape would only work when the option is close to be at the money, i.e., the strike price is approximately equal to the spot price. In this case, the simple moneyness, m, is close to 1, making $log(m)$ close to 0.

Using a Taylor expansion, we can approximate the implied moneyness, M, by a polynomial of m and τ. The advantage of doing this is not only due to computational efficiency but also it can resolve the problem, where

$$\log M \to -\infty \ as \ M \to 0$$

i.e., when the strike price is way less than the spot price (for deep out-of-money put options or deep in-the-money call options), the regression model proposed by Roux will generate unpredictable behaviours and this is the reason why the model will not work well for those options.

As a result, we propose a new model consists of degree three polynomials of m and τ, with the first variation that excluding the VIX as an explanatory variable. This means that the entire implied volatility is specified as:

Model 6a: $\sigma_t(\hat{m}_t, \tau) = p_{00,t} + p_{10,t}\hat{m}_t + p_{01,t}\tau_t + p_{20,t}\hat{m}_t^2 + p_{11,t}\hat{m}_t\tau_t + p_{02,t}\tau_t^2 + p_{30,t}\hat{m}_t^3 + p_{21,t}\hat{m}_t^2\tau_t + p_{12,t}\hat{m}_t\tau_t^2 + p_{03,t}\tau_t^3 + \epsilon_t$

where σ is the implied volatility, $p_{xx,t}$ is the corresponding parameters of m and τ terms, m is defined as the simple moneyness, i.e., strike over spot and τ is simply the time to maturity in years, assuming 365 days in a year.

The second variation of the model is closer to the Model 5 proposed by Roux, which models the residual of implied volatilities after VIX is being subtracted:

Model 6b: $\sigma_t(\hat{m}_t, \tau) - VIX_t = p_{00,t} + p_{10,t}\hat{m}_t + p_{01,t}\tau_t + p_{20,t}\hat{m}_t^2 + p_{11,t}\hat{m}_t\tau_t + p_{02,t}\tau_t^2 + p_{30,t}\hat{m}_t^3 + p_{21,t}\hat{m}_t^2\tau_t + p_{12,t}\hat{m}_t\tau_t^2 + p_{03,t}\tau_t^3 + \epsilon_t$

where the symbols are defined similar to that of Model 6a and VIX index is just the mid-price (the average of high and low prices) on that particular day.

Although the fitted coefficient of Model 6a and Model 6b are different due to the use of different dependent variable in the respective regressions, Model 6b is essentially Model 6a with a downward parallel shift of the entire surface for a particular day by the amount of VIX index on that day. This is because we are using only the mid-price of the VIX index on each day and hence subtracting all implied volatility on that day by the same number.

Since Models 1 to 4 use implied moneyness M, instead of simple moneyness m, we have included the implied moneyness as part of the consideration and proposed Model 7, which is similar to Model 6 except M is used in place of m.

Model 7: $\sigma_t(\hat{M}_t, \tau) = p_{00,t} + p_{10,t}\hat{M}_t + p_{01,t}\tau_t + p_{20,t}\hat{M}_t^2 + p_{11,t}\hat{M}_t\tau_t + p_{02,t}\tau_t^2 + p_{30,t}\hat{M}_t^3 + p_{21,t}\hat{M}_t^2\tau_t + p_{12,t}\hat{M}_t\tau_t^2 + p_{03,t}\tau_t^3 + \epsilon_t$

All other symbols are defined similarly as before, except the implied moneyness, which is defined as:

$$M = \frac{-r\tau - \log m}{\sqrt{\tau}}$$

in place the simple moneyness m.

The last extension we propose resembles closely the original Roux model, however we have added the higher-degree terms in an attempt to better model the shape of the implied volatility surface:

Model 8: $\sigma_t(\hat{m}_t, \tau) = p_{00,t} + p_{10,t} \log(\hat{m}_t) + p_{01,t} \frac{1}{\sqrt{\tau}_t} + p_{20,t} (\log(\hat{m}_t))^2 + p_{11,t} \log(\hat{m}_t) \frac{1}{\sqrt{\tau}_t} + p_{02,t}(\frac{1}{\sqrt{\tau}_t})^2 + p_{30,t}(\log(\hat{m}_t))^3 + p_{21,t}(\log(\hat{m}_t))^2 \frac{1}{\sqrt{\tau}_t} + p_{12,t}(\log(\hat{m}_t))(\frac{1}{\sqrt{\tau}_t})^2 + p_{03,t}(\frac{1}{\sqrt{\tau}_t})^3 + \epsilon_t.$

3.3 Using promptness in parametric models

Another direction to extend the current research is to use the promptness instead of the absolute time to maturity, which is a concept that is frequently used in commodities trading. This is particularly sensible during the low-interest rate regime which is currently experienced by the western world in the aftermath of the recent financial crisis. For instance, the Federal Funds Target Rate, which is typically regarded as the benchmark interest rate for US economy, has been around 0.25% for the past few years, as shown in Figure 3.10.
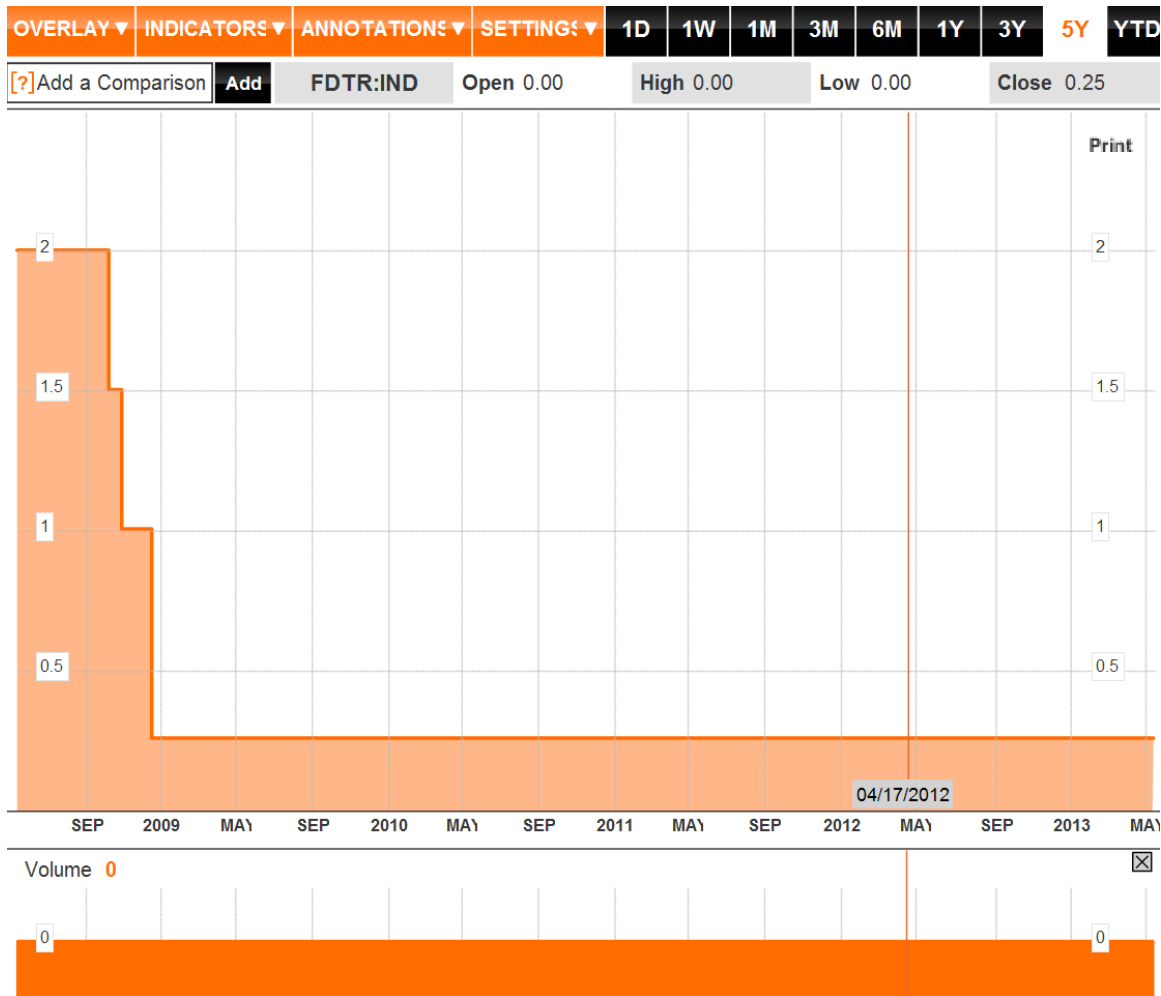
Figure 3.10: S&P500 Historical Fed's Funds Target Rate, Courtesy of Bloomberg.com

As such the impact of the time value of money of options is rather minimal within a relatively short period of time.

Therefore the evolution of implied volatilities of the options within the same promptness should remain more or less the same. For instance, the plot below shows the evolution of implied volatilities versus moneyness (strike price over spot price) of out-of-money options for different promptness from March 11 2013 to March 22, 2013:
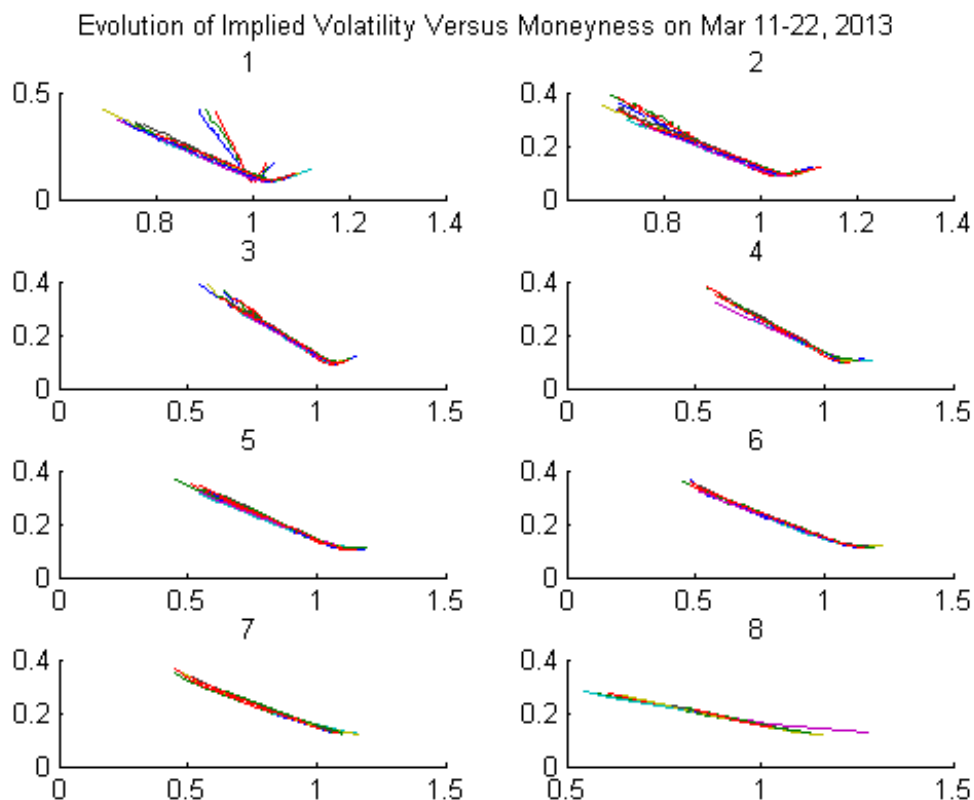
Figure 3.11: Evolution of Implied Volatility of Out-of-money Options Versus Moneyness, Mar 11, 2013 to Mar 22, 2013

On top of each subplot is the promptness of the options being quoted, with 1 being the first prompt (i.e., the first option to expire) and 8 being the furthest prompt being quoted and traded (i.e., options expiring in about 8 months' time). As we will discuss further in the next section, options that are very far away from maturity are very thinly traded and hence are excluded from our analysis.

Each curve represents the implied volatility at various moneyness on a particular trading day. From the graph, we can see that other than some drastic fluctuations of the first prompt options during the few days around expiration (the last trading day of the March 2013 option was on March 15, 2013, which falls right in the middle of this interval), the implied volatility curves generally show little changes in shape, even after the promptness has rolled over such as when options expiring for April 2013 have become the first prompt option rather than the March 2013 options after March 15.

Note that this does not only hold in relatively less volatile periods in the market. Such observations can also be made during the periods where the market is relatively more volatile. Figure 3.12 shows the evolution of implied volatility versus moneyess of out-of-money options around May 21, 2010, when VIX index was at a relatively high point of 48.2:
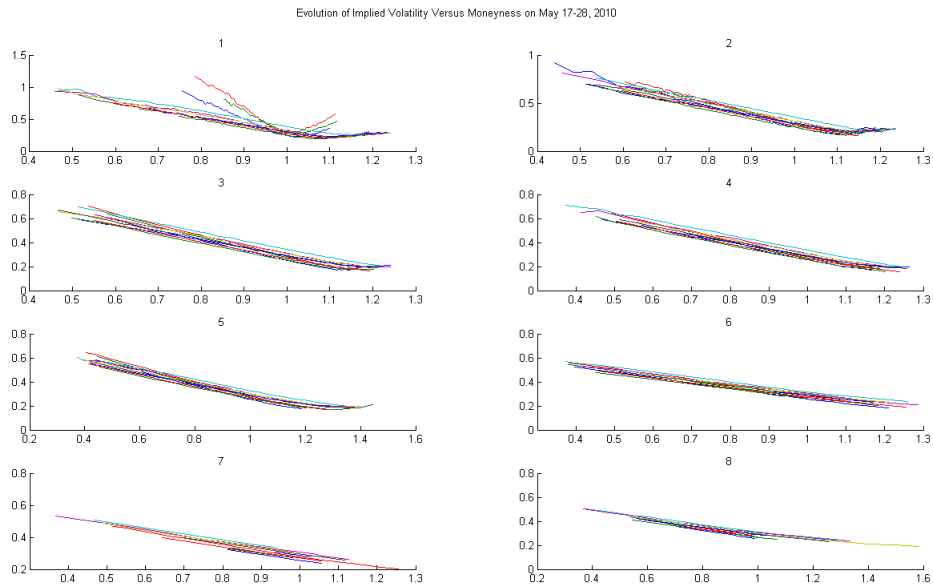
Figure 3.12: Evolution of Implied Volatility of Out-of-money Options Versus Moneyness, May 17, 2010 to May 28, 2010

However, such a trend seems to break down completely during the time of extremely high volatility. Figure 3.13 shows what happens between October 20 2008 to October 31, 2008, when VIX index reached all-time historical high of 96.4 during this period:
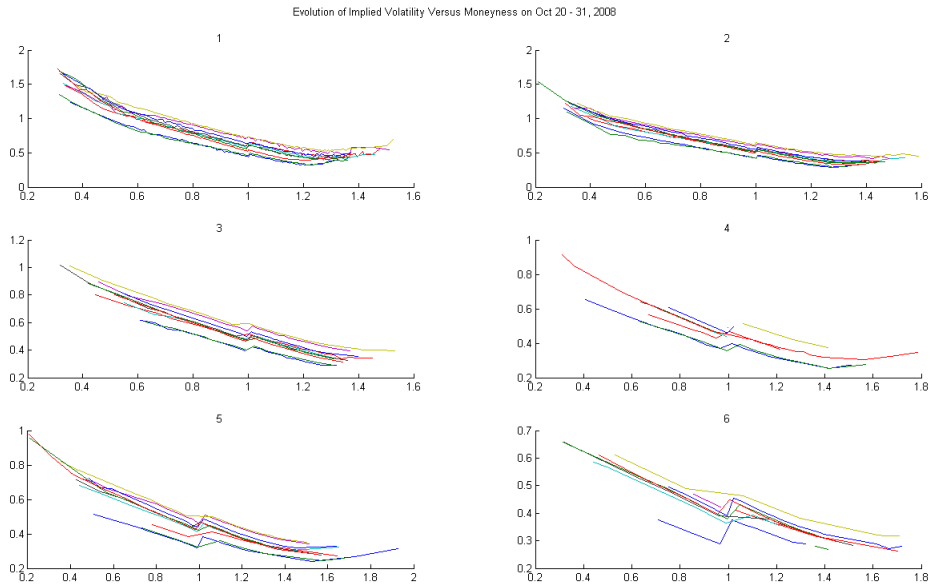
Figure 3.13: Evolution of Implied Volatility of Out-of-money Options Versus Moneyness, Oct 20, 2008 to Oct 31, 2008

Note that on the graph above, there are significantly less data points available (2427 implied volatility values for the October 2008 plots versus 3142 data points for the plots for May 2010). This is due to the fact that any implied volatility quoted without any trading volume on that day is not recorded. This could cause visual distortion in the graphs. The differences in data points are even more obvious for options with longer expiration (higher promptness), since at such a volatile market condition, it is very difficult to trade the long-dated options as few investors would take the risk of speculating the movements of the markets for an extended period of time.

Furthermore, the series of the graphs above are just for out-of-money options (both call options and put options); however, when plotted against all moneyness for either call or put options, the graphs look somewhat differently:
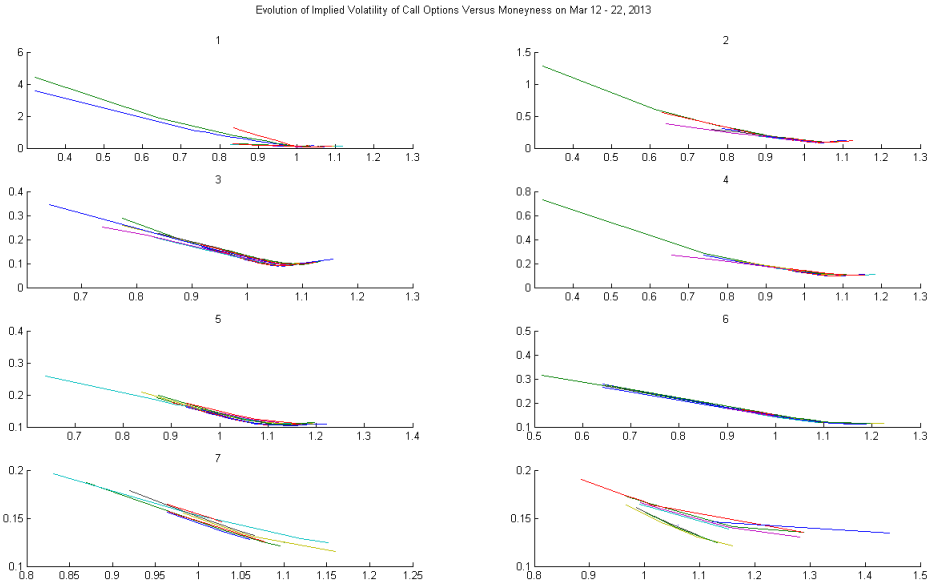
Figure 3.14: Evolution of Implied Volatility of Call Options Versus Moneyness, Mar 11, 2013 to Mar 22, 2013

Figure 3.14 shows the implied volatilities versus moneyness plot for call options of SPX from March 11 to March 22, 2013, for both in-the-money and out-of-money call options. In this graph moneyness is defined to be:

$$m = \frac{K}{S_t}$$

As such, when moneyness is less than 1, the options are in the money and when moneyness is greater than 1, the options are out-of-money. Obviously when moneyness is greater than 1, the graph is the same as Figure 3.11. However when moneyless is less than 1, the lines are far apart, indicating that the implied volatilities are no longer consistent for the same promptness.

The plot below shows that the implied volatilities of put options are graphed against moneyness for both in-the-money and out-of-money put options for the same period as Figure 3.14:
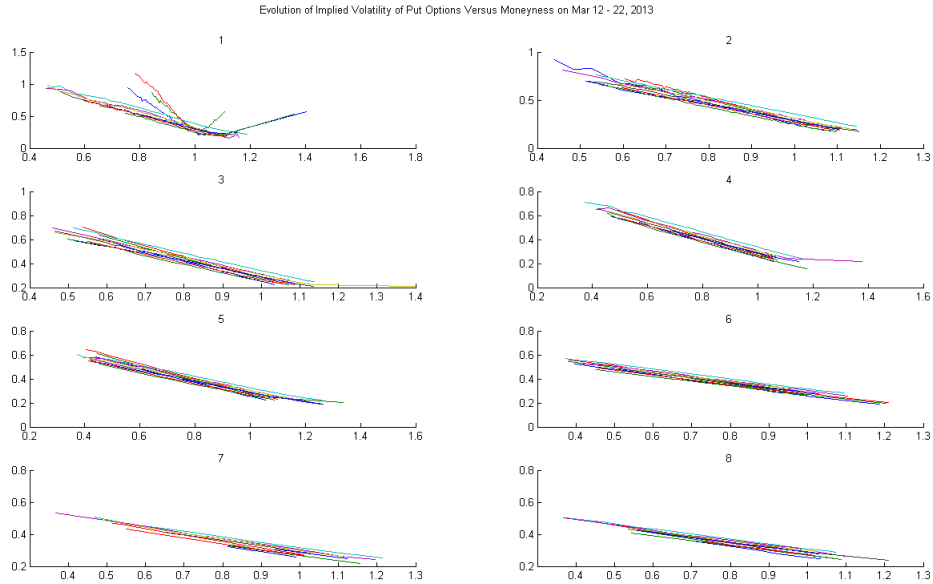
Figure 3.15: Evolution of Implied Volatility of Put Options Versus Moneyness, Mar 11, 2013 to Mar 22, 2013

Notice that when moneyness is less than one, the options are out-of-money and vice-versa. However, it is interesting to note that for put options, the in-the-money options are showing smaller movements than the out-of-money options. Overall the changes in implied volatility for put options are less than the changes in call options.

The models using promptness are similar to the models proposed above, with the exception of having promptness in place of time to maturity, τ. By using promptness, we hope to achieve more robust fitting results in which the surface does not have to be recalibrated everyday. Further details of this argument will be discussed in the later section together with the empirical results.

3.4 Data description

Data selection is of particular importance to the regression process. For the purpose of this thesis, we choose the monthly options of S&P500 index (SPX) for our analysis (there are also weekly and quarterly index options quotes available which could be used for further research into this topic). Although the results may be applicable to the volatility

surfaces of other underlying assets, the S&P 500 index represents the large-cap stocks of the US equity markets and is, in general, regarded as an indicator for the movements of the US stock markets. As such, the liquidity of the S&P 500 index option is often regarded as one of the highest since many investors use it as a proxy for the US equity markets.

The implied volatilities are extracted directly from the out-of-money index options at various strike levels, in order to construct the observed volatility surface. However, options at certain strike levels are not actively traded and have zero volume. Although the price is being quoted by the market-makers, they are not good indicators of the actual implied volatility of the options in the eyes of the investors. Hence, for options without any trading volume, the "artificially" quoted implied volatilities are ignored.

Overnight USD-LIBOR rates are being used as the risk-free interest rates where applicable. This is consistent with the industrial practice.

The VIX index is taken directly from the historical data with no filtering. Furthermore, in determining the stressed and non-stressed periods, VIX index is used as the sole determinant. Subrahmanyam [26] proposes a more complicated market sentiment determinant named "BW Sentiment Index" which could potentially be used as an extension of this thesis.
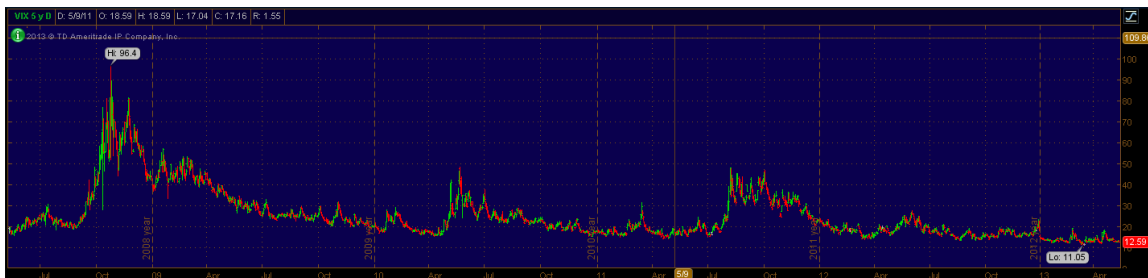
Figure 3.16: Historical VIX Index

From Figure 3.16, we could easily observe that over the past five years, VIX index was high during the following period, which are classified as the stressed periods for the purpose of our research:

- Period around October 23, 2008, when VIX index reached an all-time high of 96.4

- Period around May 21, 2010, when VIX reached 48.2 during the day

- Period around August 8, 2011, when VIX reached 48 during the day

A few other periods are chosen as the non-stressed periods. We also include one of the most recent periods as the non-stressed period as well:

- Period around August 17, 2012, when VIX reached 13.3 during the day

- Period around February 15, 2013, when VIX reached 12.24 during the day

- Period around March 14, 2013, when VIX reached the 5-year low level of 11.05 during the day

For each of the periods, we use two trading-weeks' worth of data to perform a number of analysis. Normally, a trading-week has 5 days, however for two of the periods covered, there was a day during each period that is a trading holiday; as such, there were only four trading days during that trading-week. However, as the regressions are run independently for each of the days, having shorter trading weeks will not cause too much of an issue here.

A common misconception is that the options that are close to maturity and/or are close to at-the-money (i.e., moneyness close to 1) are more heavily traded than the options which are not. This seems to hold only during the relatively "calm" periods, i.e., periods when VIX index is relatively low.

The following series of graphs are used to illustrate this idea, which uses the trading volume of S&P500 options at different periods of time, for various strikes and time to maturity.

The first example is on March 19, 2013, when the VIX index was 12.92 at the lowest point of the day:
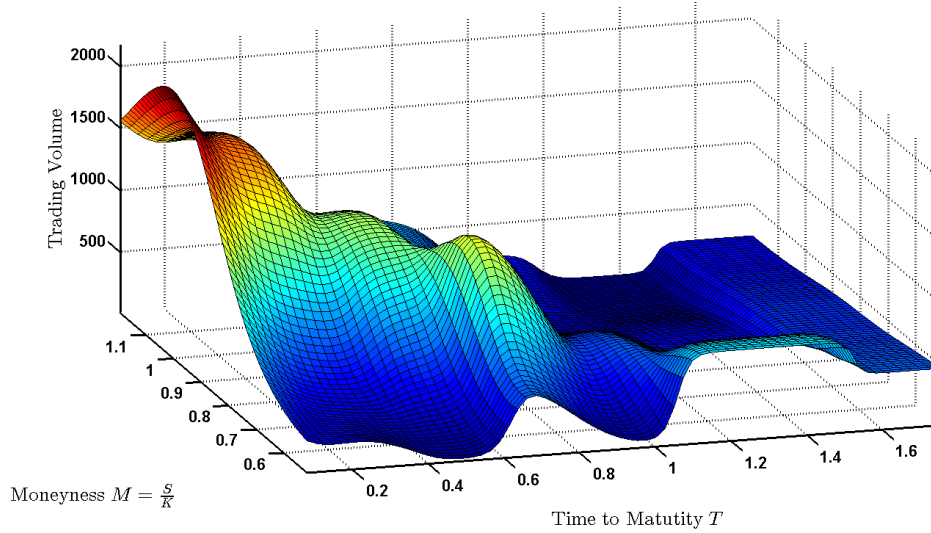
Figure 3.17: SPX Option Trading Volume on March 19, 2013

Another example is given by the plot on February 19, 2013, when the VIX index was at 12.08 during the day:
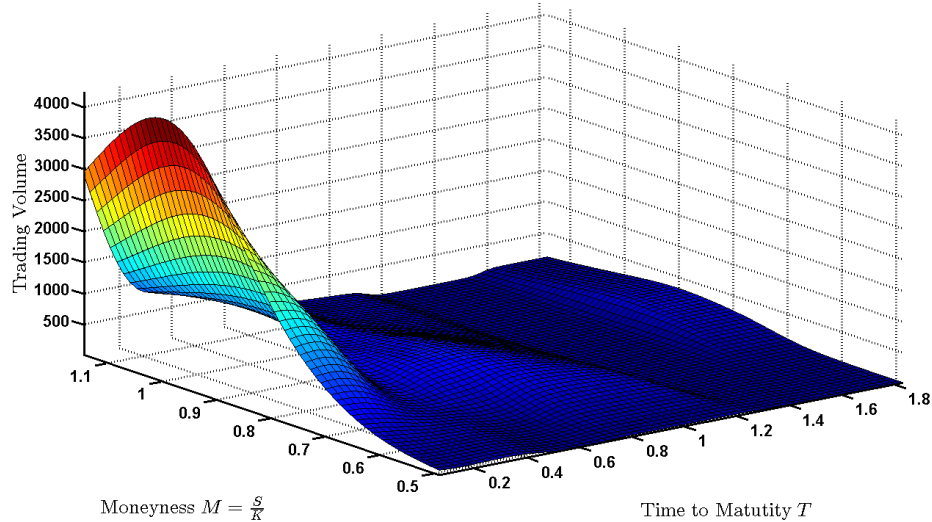
Figure 3.18: SPX Option Trading Volume on Feb 19, 2013

Note that in both of the two cases above, options with time to maturity close to zero and moneyness close to one are the most actively traded options.

41

On the other hand, in the periods where VIX index is high, such as around October 23, 2008, when VIX was at the all-time historical high of 96.14, the most actively traded options are neither the first ones to expire nor very close to at-the-money.
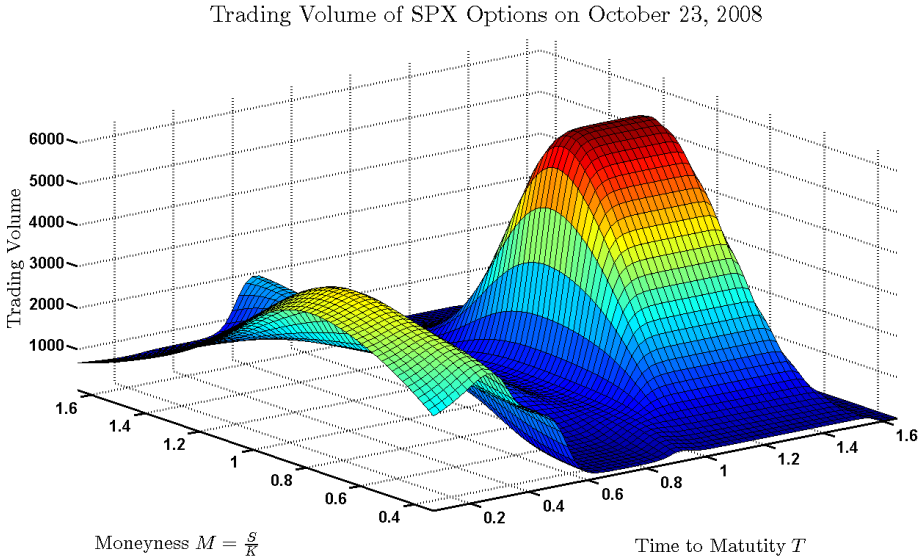
Figure 3.19: SPX Option Trading Volume on October 23, 2008

Another example is given by the plot of the trading volume against maturity and moneyness of the SPX options on October 29, 2008, when VIX index was trading at a high level of 71.14:
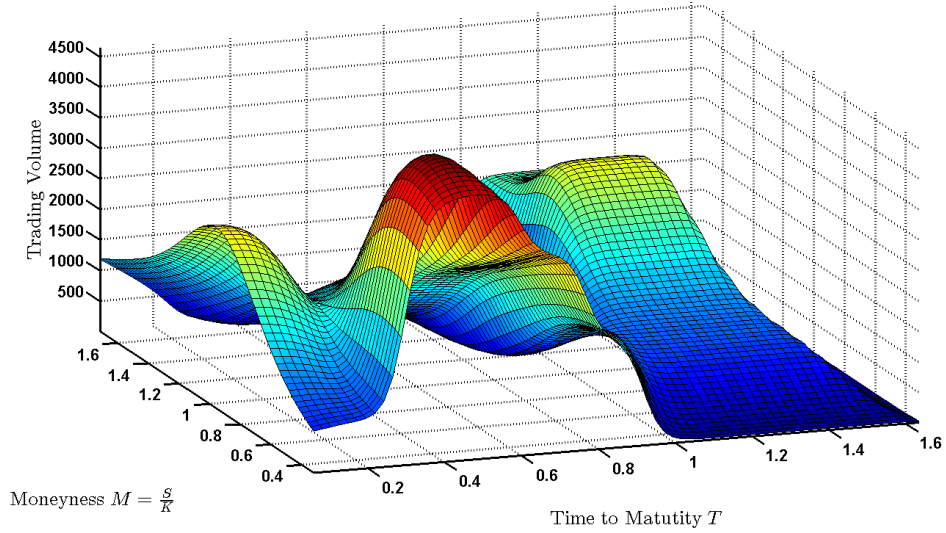
Figure 3.20: SPX Option Trading Volume on October 29, 2008

Even at a time of extremely low volatility, for example, on March 14, 2013, when the VIX index was at a 5-year low of 11.05 during the intra-day trading, the most actively traded option, although close to at-the-money, is not the option with the shortest maturity:
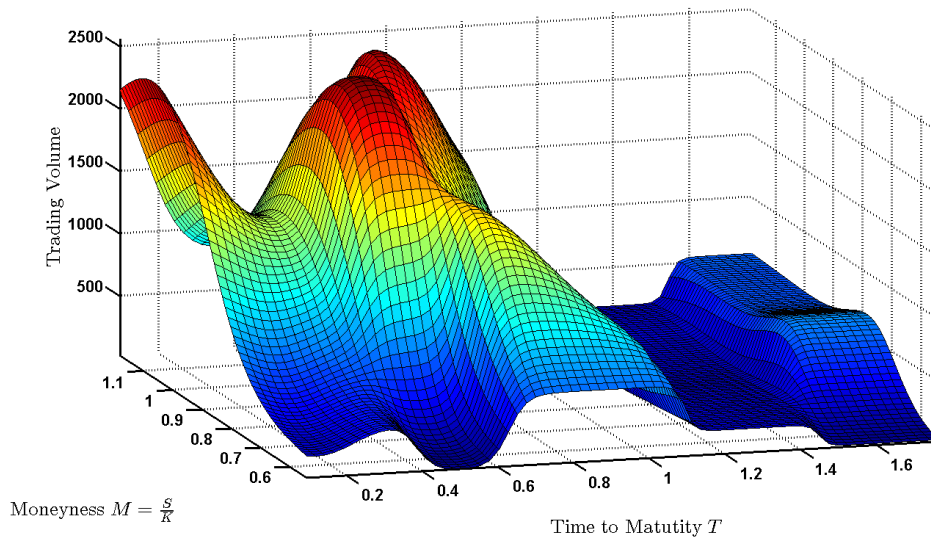
Figure 3.21: SPX Option Trading Volume on March 14, 2013

Ideally, the regression models should fit well at all maturities and moneyness levels, since the cases when moneyness is close to 0 or when time to maturity is 0 is non-trivial.

3.5 Surface fitting methodology

The regression analysis is carried out straightforwardly by using non-linear least square fitting methods. The goal of solving a non-linear least square fitting is to find a set of parameters that minimizes the sum of squared errors:

$$\min(\sum_{i=1}^{n}(\sigma_{BS}^{i}(X,\tau) - \sigma_{fitted}^{i}(X,\tau))^2)$$

where

- n = number of observations,

- $\sigma_{BS}^{i}(X,\tau)$ = the ith observed value of the implied volatility, using Black-Scholes model,

- $\sigma_{fitted}^{i}(X,\tau)$ = the ith fitted value, using the regression model, where X is the moneyness or strike values depending on the models used.τ is the time to maturity of the ith observation.

It would be very laborious to search for the set of parameters that fits such a criterion by trial and error, if that is at all possible. Fortunately we can use a matrix algebra representation for the non-linear regression problem.

Essentially, using the matrix approach, the curve fitting problem can be recast as the following system of equation:

$$AX = B$$

where

- A = matrix of independent variables,

44

- B = vector dependent variables,

- X = coefficient matrix.

Multiplying A^T on both sides, we have:

$$A^T A X = A^T B.$$

Since the matrix $A^T A$ is a square matrix that is assumed to be invertible, we can multiply $(A^T A)^{-1}$ on both sides of the equation to obtain the least square coefficient:

$$X = (A^T A)^{-1} A^T B$$

In Roux's model, the author uses a weighted scheme to fit the surface, where the weight used is σ_{imp}^{-1}, with σ_{imp} being the implied volatility. The author argues that high implied volatilities are related to deep out-of-money (or in-the-money) options, and they are thinly traded. This scheme obviously has its merits; however, as we have observed in the volume plots in Section 3.4 (more specifically Figures 3.17-3.21), it is quite evident that the actively traded options are not just restricted to the options that are close to at-the-money. This is true particularly for some of the long-dated options, where options that are relatively deep out-of-money are traded quite actively as well. Furthermore, by assigning smaller weights to the options whose strike prices are further away from spot prices, the model may have a better fit for the options that have strike prices close to spot prices; but for the options that are not, the fit would be worse than the equal-weighted scheme. Motivated by this argument, we adopt both the equally-weighted scheme as well as the observed implied volatility weighted scheme in the analysis.

The methodology for implementing the weighted scheme is carried out by using the *fminsearch* function in Matlab, which performs an unconstrained non-linear optimization, i.e., finding the set of parameters that would minimize the following objective function:

$$\min(\sum_{i=1}^{n} W_i (\sigma_{BS}^i(X, \tau) - \sigma_{fitted}^i(X, \tau))^2)$$

where W_i is the weight assigned for the ith observation and other symbols are defined in the same way as in the unweighted scheme.

One of the key issues arises in solving an unconstrained nonlinear optimization problem is the choice of initial values. Fortunately, the parameters obtained from the unweighted scheme can naturally serve as a set of initial values to solve for the parameters of the weighted scheme. In the actual implementation, the data for each period is fitted using the unweighted scheme, and the average of the coefficients obtained for each period is used as the initial value of the weighted scheme.

The curve fitting is done separately for each of the Models 1-8 and for each of the six periods selected, for both unweighted scheme, with one set of parameters and the relevant statistics recorded for that day.

3.6   Empirical results and analysis

In this section, for each fitting method, we would first report a set of regression coefficients from Model 7 in one of the periods with high VIX index level, as well as the mean, standard deviation and 95% confidence intervals. Next we report some of the relevant statistics associated with the model using the empirical data. The same exercise is then repeated for the same model during one of the periods with low VIX index level. After that, we look at the overall statistics for all of the models we consider.

3.6.1   Statistical results using unweighted fitting scheme

Regression coefficients and statistics for Model 7 using unweighted fitting scheme in high- and low-volatility regimes

First, the equal-weighted scheme is used and below are the regression results using Model 7 and the relevant statistics, for the period from October 20 to October 31, 2008, which is one of the periods with relatively high VIX levels. The 95% confidence intervals are constructed by assuming that the random variable of coefficients in the regression models

follows a normal distribution.

Table 3.1: Regression Coefficients for Model 7 Using Implied Volatility Data Between Oct 20, 2008 and Oct 31, 2008 using Unweighted Scheme

Date	p00	p10	p01	p20	p11	p02	p30	p21	p12	p03
20-Oct-08	0.54765	0.20931	0.04318	0.02429	0.18103	0.27301	-0.00819	-0.02227	-0.23219	-0.31557
21-Oct-08	0.54796	0.18536	-0.09416	0.01922	0.11630	0.24276	-0.00262	-0.03523	-0.17697	-0.17886
22-Oct-08	0.71663	0.20993	-0.66076	0.03576	-0.02476	0.78382	-0.00637	-0.14941	-0.22897	-0.36603
23-Oct-08	0.69926	0.21332	-0.50908	0.02473	0.05968	0.65196	-0.00492	-0.06615	-0.16710	-0.29861
24-Oct-08	0.82202	0.21764	-0.74065	0.02232	0.12531	0.99421	-0.00676	-0.13881	-0.51036	-0.69676
27-Oct-08	0.83980	0.22007	-0.99561	0.03449	0.08709	1.67477	-0.01043	-0.11711	-0.23925	-0.87676
28-Oct-08	0.68751	0.22862	-0.41019	0.01052	0.00483	0.57191	-0.00171	-0.03452	-0.09730	-0.26275
29-Oct-08	0.72724	0.20800	-0.55338	0.00645	0.12217	0.84253	-0.00114	-0.02425	-0.19056	-0.42544
30-Oct-08	0.63936	0.17898	-0.54069	0.01875	0.30833	0.98255	-0.00092	-0.08099	-0.42081	-0.59671
31-Oct-08	0.57772	0.16736	-0.44742	0.02966	0.28192	0.76033	-0.00339	-0.08440	-0.24751	-0.39155
Avg	0.68052	0.20386	-0.49088	0.02262	0.12619	0.77779	-0.00464	-0.07532	-0.25110	-0.44090
St Dev	0.10369	0.01981	0.29884	0.00946	0.10750	0.40786	0.00323	0.04733	0.12333	0.21714
95% CI Lower	0.61625	0.19158	-0.67609	0.01676	0.05956	0.52499	-0.00665	-0.10465	-0.32754	-0.57549
95% CI Upper	0.74478	0.21614	-0.30566	0.02848	0.19282	1.03058	-0.00264	-0.04598	-0.17467	-0.30632

Table 3.2 shows relevant statistics, which are

- **SSE**: sum of squared error,

- **RSquare**: coefficient of determination,

- **Dfe**: degree of freedom,

- **adjrsquare**: Adjusted R-squared,

- **rmse**: root mean squared error.

Table 3.2: Relevant Statistics for Model 7 Using Implied Volatility Data Between Oct 20, 2008 and Oct 31, 2008 using Unweighted Scheme

Date	sse	rsquare	dfe	adjrsquare	rmse
20-Oct-08	0.11129	0.98294	220	0.98224	0.02249
21-Oct-08	0.09996	0.98285	213	0.98212	0.02166
22-Oct-08	0.17996	0.98471	283	0.98423	0.02522
23-Oct-08	0.15061	0.98623	255	0.98575	0.02430
24-Oct-08	0.14948	0.98453	207	0.98385	0.02687
27-Oct-08	0.14955	0.98779	232	0.98731	0.02539
28-Oct-08	0.08576	0.99434	278	0.99415	0.01756
29-Oct-08	0.13174	0.98971	271	0.98936	0.02205
30-Oct-08	0.09145	0.99287	233	0.99259	0.01981
31-Oct-08	0.19939	0.98558	270	0.98510	0.02717
Mean	**0.13492**	**0.98715**	**246**	**0.98667**	**0.02325**

and another example which fits the same model using the equal-weighted scheme, but to the data for the March 2013 period, which is one of the non-stress periods that we have identified:

Table 3.3: Regression Coefficient for Model 7 Using Implied Volatility Data Between March 11, 2013 and March 22, 2013 using Unweighted Scheme

Date	p00	p10	p01	p20	p11	p02	p30	p21	p12	p03
11-Mar-13	0.10884	0.12899	0.11841	0.27548	0.31516	-0.03728	-0.16478	-0.30790	-0.18274	0.00285
12-Mar-13	0.11225	0.16603	0.12366	0.22497	0.22535	-0.05138	-0.14442	-0.25725	-0.12393	0.00901
13-Mar-13	0.10492	0.13768	0.17348	0.23806	0.35179	-0.12387	-0.14336	-0.31014	-0.19548	0.03573
14-Mar-13	0.10139	0.17110	0.13962	0.30421	0.19929	-0.05972	-0.23420	-0.35020	-0.08274	0.01143
15-Mar-13	0.10179	0.17001	0.15135	0.26930	0.25007	-0.07167	-0.20311	-0.31895	-0.14335	0.01225
18-Mar-13	0.11966	0.20228	0.14422	0.13826	0.11546	-0.08999	-0.10054	-0.17776	-0.04262	0.02496
19-Mar-13	0.12737	0.21903	0.10288	0.16630	0.11009	-0.02786	-0.16188	-0.21648	-0.04016	0.00188
20-Mar-13	0.11047	0.18900	0.15953	0.13446	0.14967	-0.10156	-0.09852	-0.16016	-0.06182	0.02785
21-Mar-13	0.12273	0.21680	0.14063	0.07455	0.08744	-0.08424	-0.07889	-0.11784	-0.03619	0.02197
22-Mar-13	0.12132	0.20046	0.12455	0.13826	0.16181	-0.05850	-0.14807	-0.16311	-0.07687	0.01252
Avg	0.11307	0.18014	0.13783	0.19639	0.19661	-0.07061	-0.14778	-0.23798	-0.09859	0.01605
St Dev	0.00922	0.03098	0.02095	0.07608	0.08896	0.02968	0.04767	0.08151	0.05928	0.01112
95% CI Lower	0.10736	0.16094	0.12485	0.14923	0.14148	-0.08901	-0.17732	-0.28850	-0.13534	0.00915
95% CI Upper	0.11879	0.19934	0.15082	0.24354	0.25175	-0.05221	-0.11823	-0.18746	-0.06185	0.02294

Table 3.4 shows the relevant statistics:

Table 3.4: Relevant Statistics for Model 7 Using Implied Volatility Data Between March 11, 2013 and March 22, 2013 using Unweighted Scheme

Date	sse	rsquare	dfe	adjrsquare	rmse
11-Mar-13	0.03948	0.98168	364	0.98123	0.01041
12-Mar-13	0.02758	0.98978	393	0.98955	0.00838
13-Mar-13	0.04145	0.98000	331	0.97946	0.01119
14-Mar-13	0.01347	0.99049	293	0.99020	0.00678
15-Mar-13	0.01200	0.99128	315	0.99103	0.00617
18-Mar-13	0.01790	0.99283	395	0.99267	0.00673
19-Mar-13	0.01096	0.99479	385	0.99467	0.00534
20-Mar-13	0.01157	0.99398	323	0.99381	0.00598
21-Mar-13	0.00749	0.99573	345	0.99562	0.00466
22-Mar-13	0.01176	0.99204	307	0.99180	0.00619
Mean	**0.01937**	**0.99026**	**345**	**0.99000**	**0.00718**

A few preliminary conclusions can be drawn, based on the sample statistics and the sample observations above:

- There are more actively traded options on each day in the March 2013 period than in the October 2008 period, as observed from the degrees of freedom. This could be due to both the improved market conditions (as indicated by a much lower level of VIX index) as well as by the increasing number of participants,

- Within the same period, the fitted coefficients more or less are in the same magnitude; however between the two periods, the coefficients change very significantly.

Also, based on the examples above, we could see that assuming that the random variable follows a normal distribution, the 95% confidence intervals do not include 0, which means that the terms are unlikely to be redundant in the model (even though the

coefficient estimates could be small); however this depends on the particular set of data and the fitted model.

Aggregated statistics for all models using unweighted fitting scheme in high- and low-volatility regimes

The above observations are informal in nature; however, in order to see if a model is well fitted, one has to take a look at the aggregated statistics, some of which are presented here. The first one is the adjusted R^2 statistic for each period for each model that the fitting is carried out.

Table 3.5: Adjusted R^2 Statistic for Models 1-8 using Unweighted Scheme

Period	Model 1	Model 2	Model 3	Model 4	Model 5	Model 6	Model 7	Model 8
200810	2.109424E-16	0.956420	0.972509	0.979948	0.983895	0.975752	0.986672	0.987400
201005	-4.218847E-16	0.930785	0.943775	0.947323	0.966140	0.926465	0.979515	0.971270
201108	1.973730E-16	0.871783	0.903686	0.932816	0.969729	0.921726	0.971488	0.975079
Avg High VIX	**-4.523131E-18**	**0.919663**	**0.939990**	**0.953362**	**0.973255**	**0.941314**	**0.979225**	**0.977916**
201208	-3.885781E-16	0.837846	0.958953	0.969084	0.957519	0.946939	0.987507	0.977787
201302	0.000000E+00	0.887260	0.976922	0.979963	0.967277	0.924881	0.989260	0.983906
201303	2.220446E-16	0.895364	0.977117	0.979814	0.974161	0.941817	0.990003	0.984154
Avg Low VIX	**-5.551115E-17**	**0.873490**	**0.970997**	**0.976287**	**0.966319**	**0.937879**	**0.988923**	**0.981949**

Below we report the adjusted R^2-statistics for the two Practitioners' Black-Scholes (PBS) models mentioned in Section 3.1, for benchmarking purposes:

Table 3.6: Adjusted R^2-statistic for PBS models using Unweighted Scheme

Period	PBSa	PBSb
200810	0.939076	0.940018
201005	0.880137	0.870307
201108	0.846020	0.829927
Avg High VIX	**0.888411**	**0.880084**
201208	0.913277	0.907751
201302	0.878438	0.865963
201303	0.908501	0.899798
Avg Low VIX	**0.900072**	**0.891171**

Note that the R^2 and adjusted R^2-statistics are actually quite similar in this case (normally the differences is within the magnitude of 0.001) due to a large number of data points available. The following conclusion can be drawn based on the adjusted R^2-statistics and by using unweighted scheme:

- During the periods of both relatively high VIX levels and low VIX levels, the three best fitting models are Models 7, 8 and 4, as indicated in Table 3.5,

- Models 7 and 8 performs better than all of the existing models, and Model 6 performs better than all but Model 4 in the existing model list,

- Other than Model 1, which is essentially the volatility surface based on the assumptions of the Black-Scholes model, every other models in the investigation fit better than the PBS models,

- In general, the models perform better in the non-stressed periods (defined as the periods with low VIX index levels) than the stressed periods. The only exception

is Models 1 and 2, which do not include a time to maturity factor. However, at the same time it is also interesting to note that among the three periods with high VIX levels we perform analysis on, the fits of the models are better during the extremely high VIX levels in October 2008 than the other periods.

The next key statistics that we look at is the root mean squared error (RMSE). RMSE is the square root of the average of the squared differences. It is defined as:

$$RMSE = \sqrt{\frac{\sum_{t=1}^{n}(vol_t - \hat{vol_t})^2}{n}}.$$

where vol_t and $\hat{vol_t}$ represent the observed and fitted values of the volatility respectively and n is the number of observations. If the model is able to fit the curve perfectly and match exactly at every single observation, then RMSE should be equal to 0, and a smaller value of RMSE indicates a better fit.

For the models that we have listed above, their respective RMSE values are summarized in Table 3.7:

Table 3.7: Summary of RMSE Statistics for Models 1 - 8 using Unweighted Scheme

Period	Model 1	Model 2	Model 3	Model 4	Model 5	Model 6	Model 7	Model 8
200810	0.206837	0.042228	0.033543	0.028641	0.025658	0.032098	0.023253	0.022459
201005	0.146989	0.037903	0.034327	0.033169	0.026721	0.037143	0.021070	0.024500
201108	0.127267	0.047215	0.040935	0.034001	0.021734	0.036866	0.021828	0.019887
Avg High VIX	**0.160364**	**0.042449**	**0.036268**	**0.031937**	**0.024704**	**0.035369**	**0.022050**	**0.022282**
201208	0.082296	0.032540	0.016305	0.014057	0.015842	0.016888	0.009124	0.011839
201302	0.069776	0.022672	0.010423	0.009735	0.012352	0.018805	0.007188	0.008642
201303	0.073618	0.023522	0.010794	0.010013	0.011396	0.016588	0.007184	0.008931
Avg Low VIX	**0.075230**	**0.026244**	**0.012507**	**0.011268**	**0.013196**	**0.017427**	**0.007832**	**0.009804**

56

as well as the two PBS models for benchmarking purposes:

Table 3.8: Summary of RMSE Statistics for PBS Models using Unweighted Scheme

Period	PBSa	PBSb
200810	0.051055	0.050734
201005	0.049458	0.051768
201108	0.051925	0.054514
Avg High VIX	**0.050813**	**0.052339**
201208	0.022836	0.023634
201302	0.024212	0.025443
201303	0.021390	0.022571
Avg Low VIX	**0.022812**	**0.023883**

The following conclusions can be drawn based on the RMSE statistics using the unweighted scheme:

- Models 7 and 8 clearly once again outperform the rest of the models in both the stressed and non-stressed periods, however, Model 5 seems to be the third best fitting model during the stressed periods, and Model 4 seems to be the third best fitting model during the non-stressed period. This is different from the conclusion drawn based on the adjusted R^2-statistic,

- Similar to the adjusted R^2-statistics, only Model 1 under-performs the PBS models in both high VIX and low VIX periods, Model 2 under-performs the PBS benchmark models during the low-stress periods but not during the high-stress periods,

- Again, the models perform better during the low-stress periods than the high-stress periods. However, the models seem to fit better during the period with the highest VIX index levels (October 2008) than during the other high-stress periods and the models also fit better during the period with the lowest VIX index level (March 2013) than during the other low-stress periods.

Based on the results of both statistics, the following conclusion can be drawn for the unweighted scheme:

- Models 7 and 8 we have proposed clearly outperform any of the existing models for the periods tested. Between the two models, Model 7 performs better than Model 8 in fitting the data.

It is also interesting to note that even though Model 6 and Model 7 are very similar, Model 6 clearly performs worse than Model 7 based on the reported statistics. This shows that using the implied moneyness will achieve better fitting than using simple moneyness, although using implied moneyness does introduce computational complexity.

3.6.2   Residual analysis using unweighted fitting scheme

In addition to the reported statistics, we can also look at graphs to see visually how the models fit the data. Similar to above, the plots for the fitted volatility surfaces using Model 5 and Model 7 are generated for comparison purposes. In order to establish a better comparison, the graphs plotted are implied volatility versus simple moneyness (defined as $m = \frac{K}{S_t}$, where K and S_t are defined at the beginning of this chapter) and time to maturity, τ. The VIX index on the day of analysis is added back to the fitted values produced by Model 5. For Model 7, the fitted data is computed using the implied moneyness, but is plotted against simple moneyness. For the fitted graph, the fitted data points are represented by the blue dots and for the raw data graph, the blue dots represent the observed implied volatilities. For each period, only four days are drawn with one trading day apart, to give a better view of the data, and the title on top of each graph shows the day the surface is representing.

Figure 3.22 is the graph generated by using the observed implied volatilities for the October 2008 period, which is a period with high level of VIX:
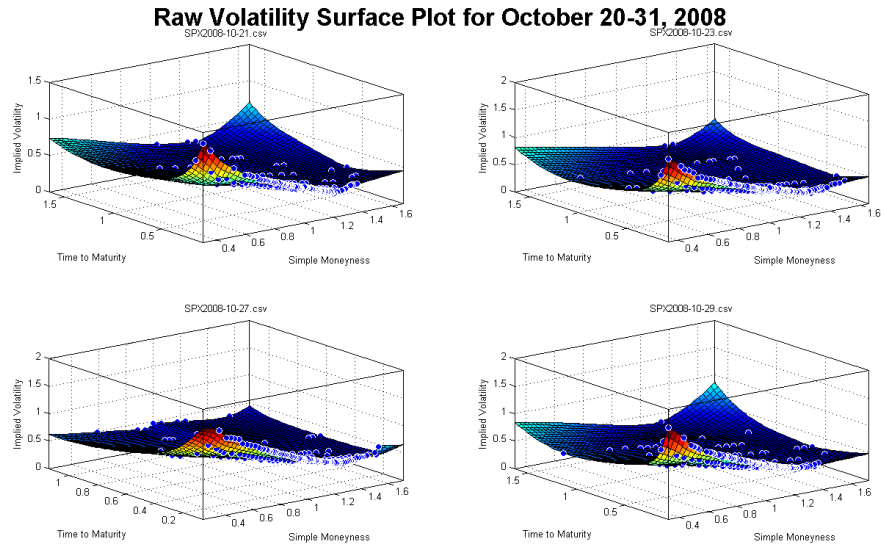
Figure 3.22: Observed Implied Volatility Surface for October 20-31, 2008

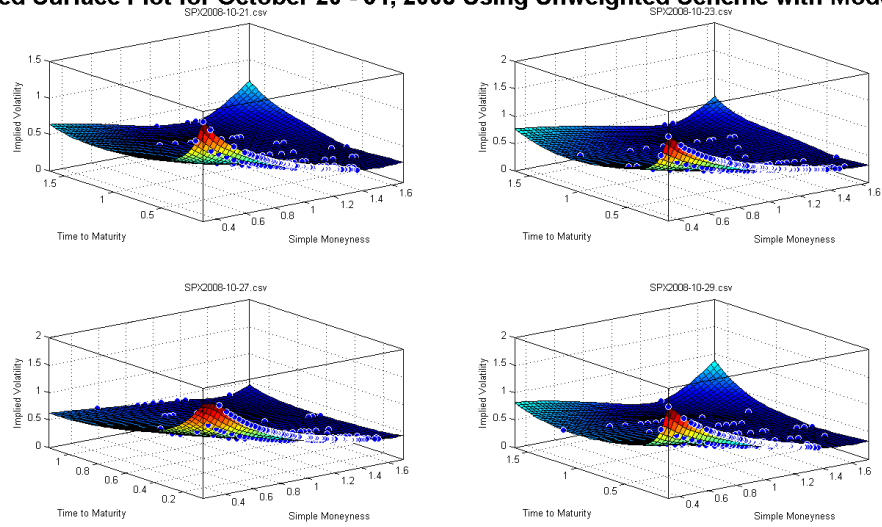The fitted graph using Model 5 for the same period is given in Figure 3.23:

Figure 3.23: Fitted Implied Volatility Surface for October 20-31, 2008 Using Model 5 with Unweighted Scheme

The plot for Model 7 is given in Figure 3.24:

Fitted Surface Plot for October 20 - 31, 2008 Using Unweighted Scheme with Model 7
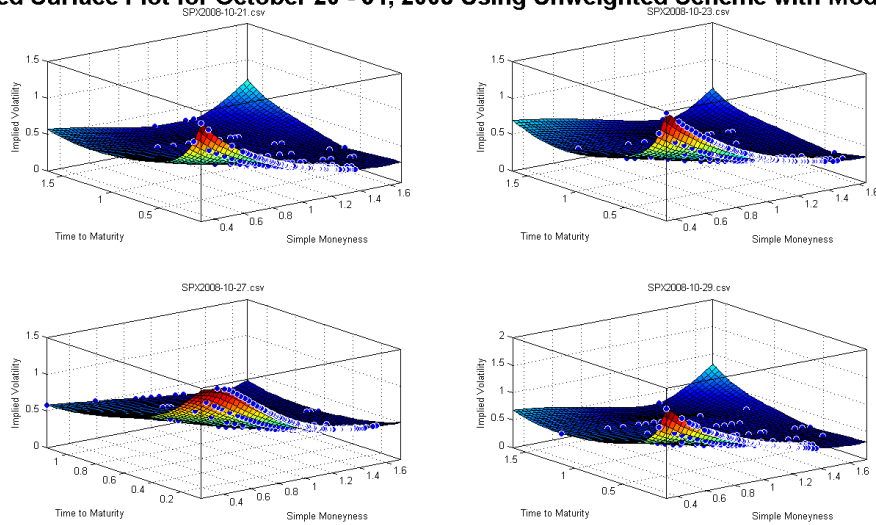
Figure 3.24: Fitted Implied Volatility Surface for October 20-31, 2008 Using Model 7 with Unweighted Scheme

Even though the differences appear to be quite small, and neither Model 5 nor Model 7 captures the curvature at the edges of the surfaces very well, we can certainly see that the curvatures in the plots using Model 7 is more visible than Model 5, particularly when looking at the parts of the graphs with large moneyness values on October 27.

The residuals of the fitted graphs are plotted against simple moneyness and time to maturity. The levels representing 10th and 90th percentile of the fitted volatility are also plotted to give some insight into the range of the data. Figure 3.25 is for the October 2008 period with data fitted to Model 5:
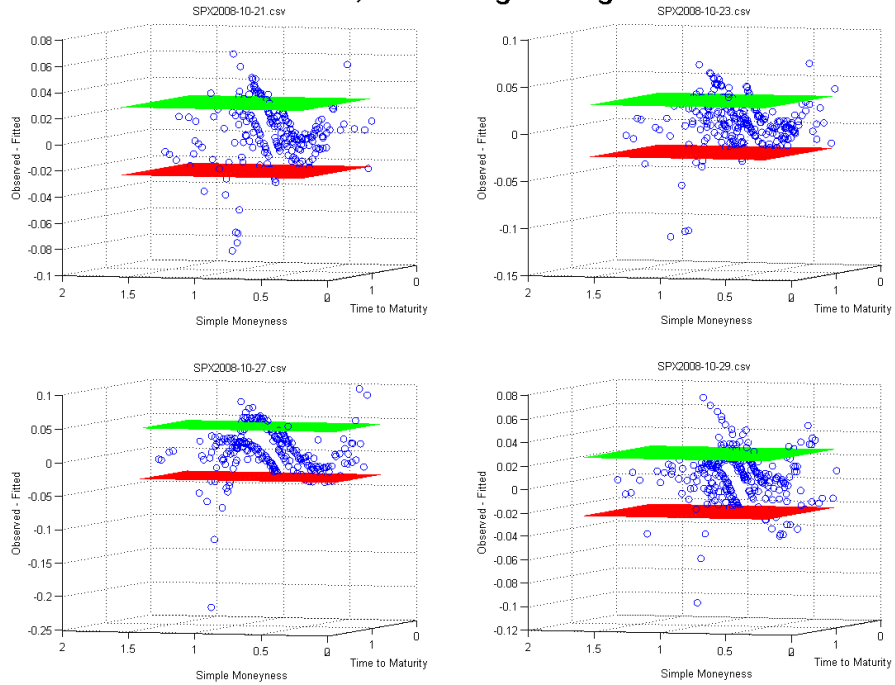
Figure 3.25: Residual Plot for October 20-31, 2008 Using Model 5 with Unweighted Scheme

Using Model 7, another set of plot is provided in Figure 3.26:

Figure 3.26: Residual Plot for October 20-31, 2008 Using Model 7 with Unweighted Scheme

All of the observed residual values seem to have centred around 0; however the 10th and 90th percentile planes are visibly narrower in the residual plots using Model 7. Narrower bands indicate that the errors are mostly within a smaller range, which is desirable.

For the period with low VIX levels, March 2013 is once again used for illustration. The observed implied volatility surface for this period is plotted in Figure 3.27:

Figure 3.27: Observed Implied Volatility Surface for March 11 - 22, 2013

The fitted surface using Model 5 and Model 7, using the unweighted scheme are shown in Figure 3.28 and 3.29 respectively:
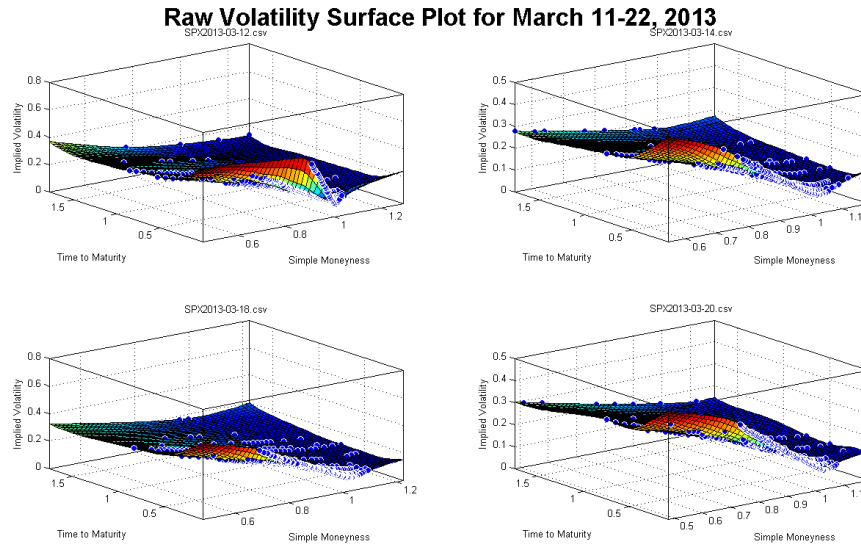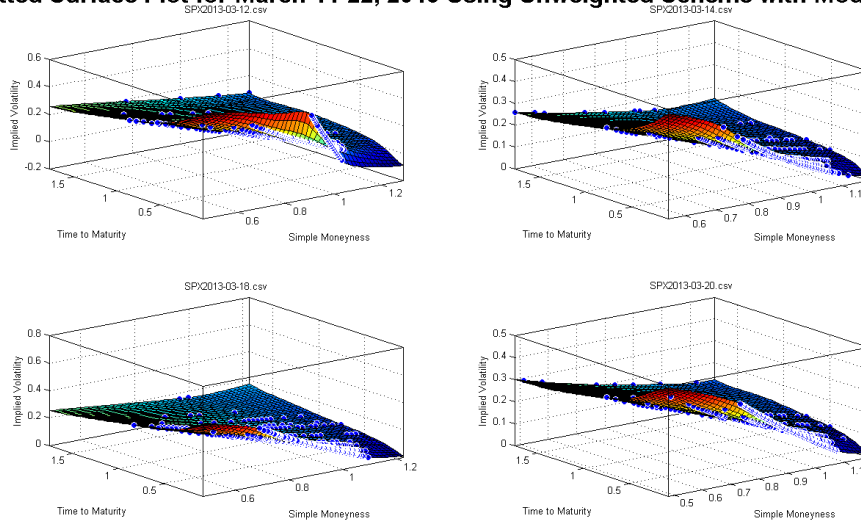

Figure 3.28: Fitted Implied Volatility Surface for March 11-22, 2013 Using Model 5 with Unweighted Scheme
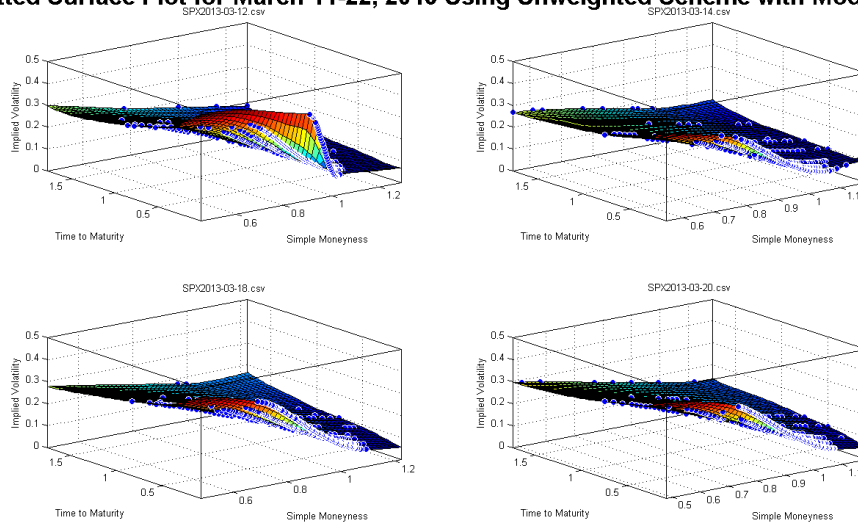
Figure 3.29: Fitted Implied Volatility Surface for March 11-22, 2013 Using Model 7 with Unweighted Scheme

On the observed implied volatility surface, there is almost always a "kink" at where the simple moneyness is one during this period, indicating discontinuities between the out-of-money call and put options. This could be explained by the fact that in the periods of relatively low volatility, more market participants are likely to make directional bets on the index levels, causing differences in the changes in volatilities between the out-of-money call and put options. In this case, once again, Model 7 shows notably more acute curvature where simple moneyness is close to one, indicating closer resemblance to the observed volatility surface. Also, and perhaps more importantly, towards the "tips" of the observed implied volatility surface, i.e., where time to maturity or simple moneyness is large, the observed volatility surface is showing an upward volatility smile while Model 5 is showing an almost downward volatility skew. Model 7, on the other hand, appears to fit much better at these extreme values.

For the March 2013 period, the residuals based on fitted data using both Model 5 and Model 7 are plotted in Figure 3.29 and 3.30 respectively:
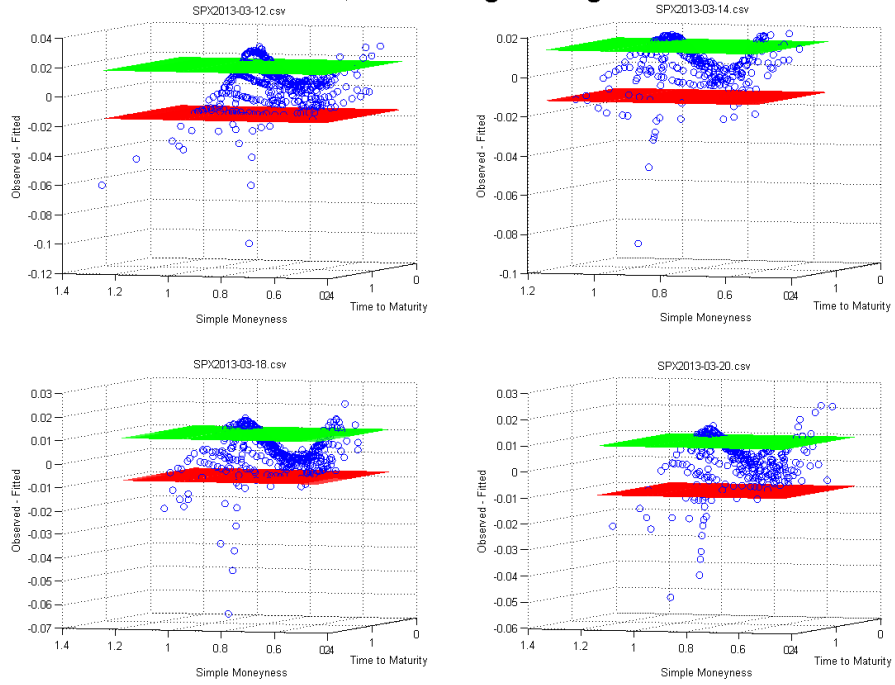
Figure 3.30: Residual Plot for March 11-22, 2013 Using Model 5 with Unweighted Scheme
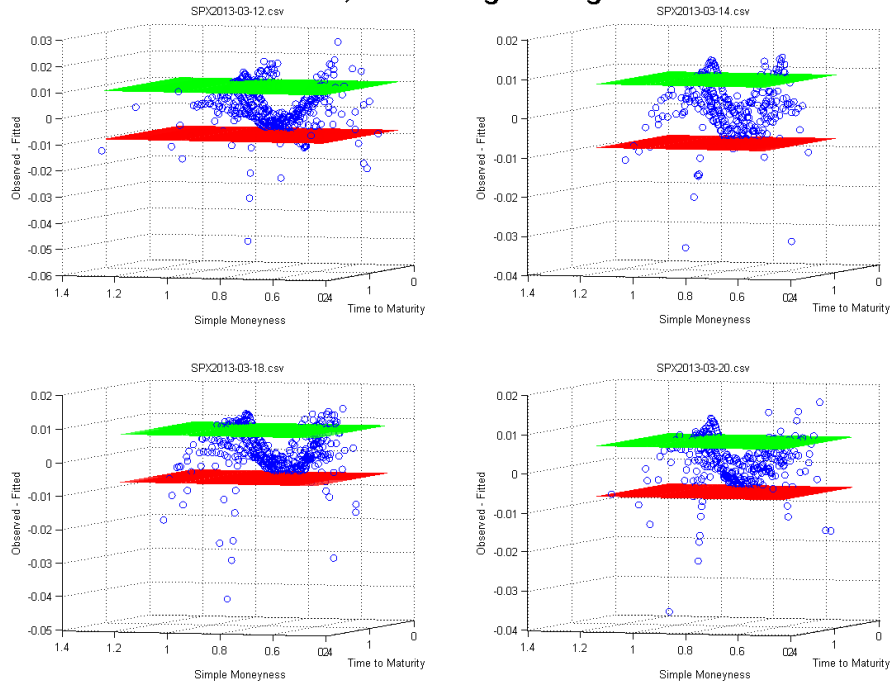
Figure 3.31: Residual Plot for March 11-22, 2013 Using Model 7 with Unweighted Scheme

Similar to the periods with high VIX levels, the band covered by the 10th and 90th percentiles are smaller in Model 7 than Model 5, indicating that Model 7 is a better fit.

The graphical observations presented above have confirmed that even though Model 5 and Model 7 both fitted relatively well to the observed volatility surfaces, Model 7 manages to capture the upward smile during the low VIX period, which is crucial in the volatility surface fitting; and has shown more acute curvatures, which is closer to the observed implied volatilities. Furthermore, the residuals of the fitted surface using Model 7 is also mostly within a smaller range compared to the residual using Model 5, which indicates a better fit.

3.6.3 Statistical results using weighted fitting scheme

Regression coefficients and statistics for Model 7 using weighted fitting scheme in high- and low- volatility regimes

The discussions above are all based on the unweighted scheme. However, as mentioned in Section 3.5, Roux has used a weighted scheme where the volatilities are fitted using the weight σ_{imp}^{-1}, where σ_{imp} is the observed implied volatilities. This fitting scheme has its merits and therefore analysis based on the fitting process using this weighted scheme are provided below as well.

For comparison purposes, we have also listed the coefficients for the two periods (October 2008 and March 2013), using the weighted scheme. Table 3.9 shows the results for the October 2008 period using Model 7 with the weighted scheme:

Table 3.9: Regression Coefficients for Model 7 Using Implied Volatility Data Between Oct 20, 2008 and Oct 31, 2008 using Weighted Scheme

Date	p00	p10	p01	p20	p11	p02	p30	p21	p12	p03
20-Oct-08	0.54374	0.21481	0.07288	0.03079	0.20966	0.26699	-0.01146	-0.04869	-0.30761	-0.36453
21-Oct-08	0.54435	0.19629	-0.07451	0.02749	0.09445	0.19869	-0.00544	-0.06594	-0.21348	-0.18196
22-Oct-08	0.70993	0.21936	-0.61608	0.04035	-0.03661	0.71565	-0.00919	-0.15769	-0.22672	-0.33856
23-Oct-08	0.69266	0.21893	-0.46183	0.02823	0.07153	0.59313	-0.00708	-0.06885	-0.18078	-0.28486
24-Oct-08	0.80952	0.23846	-0.62296	0.02560	-0.02101	0.65743	-0.00924	-0.13861	-0.32353	-0.41268
27-Oct-08	0.83726	0.22778	-0.97064	0.03596	0.09110	1.63193	-0.01242	-0.11073	-0.23997	-0.86190
28-Oct-08	0.67969	0.22620	-0.38318	0.01909	0.06318	0.59883	-0.00401	-0.04925	-0.16305	-0.31589
29-Oct-08	0.71974	0.21236	-0.50300	0.01151	0.12637	0.76551	-0.00298	-0.02970	-0.19359	-0.39180
30-Oct-08	0.63747	0.18161	-0.54766	0.02228	0.29547	1.01926	-0.00178	-0.09034	-0.40784	-0.61926
31-Oct-08	0.57093	0.17067	-0.44506	0.03756	0.28397	0.79607	-0.00580	-0.08677	-0.25763	-0.42563
Avg	0.67453	0.21065	-0.45520	0.02788	0.11781	0.72435	-0.00694	-0.08466	-0.25142	-0.41971
St Dev	0.10248	0.02140	0.29053	0.00885	0.11411	0.40008	0.00358	0.04100	0.07542	0.19187
95% CI Lower	0.61101	0.19738	-0.63527	0.02240	0.04709	0.47638	-0.00916	-0.11007	-0.29816	-0.53863
95% CI Upper	0.73804	0.22391	-0.27513	0.03337	0.18853	0.97231	-0.00472	-0.05924	-0.20468	-0.30079

Table 3.10 gives corresponding statistics:

Table 3.10: Relevant Statistics for Model 7 Using Implied Volatility Data Between Oct 20, 2008 and Oct 31, 2008 using Weighted Scheme

Date	sse	rsquare	dfe	adjrsquare	rmse
20-Oct-08	0.11506	0.98888	220	0.98842	0.02287
21-Oct-08	0.10425	0.98863	213	0.98815	0.02212
22-Oct-08	0.18794	0.98884	283	0.98849	0.02577
23-Oct-08	0.15584	0.98945	255	0.98908	0.02472
24-Oct-08	0.16406	0.98653	207	0.98595	0.02815
27-Oct-08	0.15680	0.98959	232	0.98918	0.02600
28-Oct-08	0.09365	0.99506	278	0.99490	0.01835
29-Oct-08	0.13747	0.99166	271	0.99138	0.02252
30-Oct-08	0.09334	0.99370	233	0.99346	0.02002
31-Oct-08	0.21662	0.98763	270	0.98722	0.02833
Mean	**0.14250**	**0.99000**	**246**	**0.98962**	**0.02389**

For comparison purposes, the regression coefficients and the statistics for one of the low VIX periods, March 2013, are given in Table 3.11 and 3.12 respectively:

Table 3.11: Regression Coefficient for Model 7 Using Implied Volatility Data Between March 11, 2013 and March 22, 2013 using Weighted Scheme

Date	p00	p10	p01	p20	p11	p02	p30	p21	p12	p03
11-Mar-13	0.10436	0.13140	0.12733	0.31591	0.33591	-0.04002	-0.20601	-0.34459	-0.20169	0.00153
12-Mar-13	0.10883	0.15968	0.12959	0.26323	0.26560	-0.04953	-0.17284	-0.30249	-0.15598	0.00559
13-Mar-13	0.10027	0.13432	0.18485	0.27209	0.38487	-0.12641	-0.16870	-0.35710	-0.22346	0.03362
14-Mar-13	0.09813	0.17390	0.14681	0.35638	0.21684	-0.06450	-0.30772	-0.39796	-0.09639	0.01256
15-Mar-13	0.09777	0.16509	0.16285	0.33150	0.29492	-0.08088	-0.27662	-0.38850	-0.17729	0.01377
18-Mar-13	0.11688	0.19577	0.14243	0.19486	0.14964	-0.07975	-0.15048	-0.22670	-0.07098	0.01914
19-Mar-13	0.12519	0.21699	0.10538	0.21011	0.13438	-0.02703	-0.21382	-0.25588	-0.05885	0.00080
20-Mar-13	0.10784	0.18377	0.16263	0.18321	0.17356	-0.10235	-0.14240	-0.19942	-0.07496	0.02789
21-Mar-13	0.12130	0.21585	0.14150	0.10746	0.09070	-0.08606	-0.11696	-0.12873	-0.03786	0.02297
22-Mar-13	0.11857	0.20086	0.12825	0.18491	0.18387	-0.05778	-0.21022	-0.19738	-0.09263	0.01108
Avg	0.10991	0.17776	0.14316	0.24197	0.22303	-0.07143	-0.19658	-0.27988	-0.11901	0.01490
St Dev	0.01001	0.03059	0.02262	0.07886	0.09469	0.02986	0.05969	0.09185	0.06512	0.01100
95% CI Lower	0.10371	0.15880	0.12914	0.19309	0.16434	-0.08994	-0.23358	-0.33680	-0.15937	0.00808
95% CI Upper	0.11612	0.19672	0.15718	0.29084	0.28171	-0.05293	-0.15958	-0.22295	-0.07865	0.02171

Table 3.12: Relevant Statistics for Model 7 Using Implied Volatility Data Between March 11, 2013 and March 22, 2013 using Weighted Scheme

Date	sse	rsquare	dfe	adjrsquare	rmse
11-Mar-13	0.04297	0.99596	364	0.99586	0.01087
12-Mar-13	0.02932	0.99774	393	0.99769	0.00864
13-Mar-13	0.04366	0.99582	331	0.99571	0.01149
14-Mar-13	0.01508	0.99802	293	0.99796	0.00717
15-Mar-13	0.01360	0.99824	315	0.99819	0.00657
18-Mar-13	0.02016	0.99836	395	0.99832	0.00714
19-Mar-13	0.01177	0.99890	385	0.99887	0.00553
20-Mar-13	0.01282	0.99867	323	0.99863	0.00630
21-Mar-13	0.00802	0.99912	345	0.99910	0.00482
22-Mar-13	0.01291	0.99835	307	0.99831	0.00648
Mean	**0.02103**	**0.99792**	**345**	**0.99786**	**0.00750**

Note that for both of the periods, the fitting statistics using the unweighted scheme appear to be better than the weighted scheme; however changes in the fitted coefficient estimates are very small in the case of the weighted scheme, compare to the changes in coefficient estimates in the unweighted scheme.

Aggregated statistics for all models using weighted fitting scheme in high- and low- volatility regimes

To further explore the effectiveness of various models using the weighted scheme, one has to look into the summary statistics. The adjusted R^2-statistics results are presented in Table 3.13.

Table 3.13: Summary of Adjusted R^2-Statistics for Models 1 - 8

Period	Model 1	Model 2	Model 3	Model 4	Model 5	Model 6	Model 7	Model 8
200810	0.189165	0.966061	0.978796	0.984638	0.987535	0.980342	0.989623	0.990425
201005	0.510987	0.966306	0.972080	0.973886	0.983687	0.961392	0.989305	0.985944
201108	0.556121	0.936753	0.952851	0.968150	0.987247	0.961605	0.986205	0.989520
Avg High VIX	**0.418758**	**0.956373**	**0.967909**	**0.975558**	**0.986157**	**0.967780**	**0.988378**	**0.988630**
201208	0.724171	0.958761	0.989215	0.991820	0.989025	0.985548	0.996637	0.993945
201302	0.778971	0.977528	0.995216	0.995831	0.993365	0.983790	0.997723	0.996242
201303	0.776974	0.978861	0.995203	0.995751	0.994616	0.987071	0.997863	0.996550
Avg Low VIX	**0.760039**	**0.971717**	**0.993211**	**0.994467**	**0.992335**	**0.985470**	**0.997408**	**0.995579**

Again the results of the two Practitioner Black-Scholes models are reported in Table 3.14 for benchmarking purposes:

Table 3.14: Summary of Adjusted R^2-Statistics for PBS Models

Adjusted $\hat{R^2}$	PBSa	PBSb
200810	0.949178	0.951261
201005	0.938017	0.933063
201108	0.925416	0.917287
Avg High VIX	**0.937537**	**0.933870**
201208	0.976775	0.975248
201302	0.974191	0.971409
201303	0.980401	0.978430
Avg Low VIX	**0.977122**	**0.975029**

Based solely on the results in Table 3.13 and 3.14, few observations can be made:

- Model 7 performs slightly worse than Model 8 during the stressed period but continues to be the best fitting model in the periods with low VIX index levels. Model 8 is the second best performing model with the weighted scheme during the low VIX period. The third-best performing model is Model 5 during the periods with high VIX index levels, but for periods with low VIX index levels, Model 4 is the third best performing model. In fact, Model 5 performs even worse than Model 4 and Model 3 during the unstressed periods,

- The models appear to fit better during the "extreme" periods, i.e., the period with the highest VIX index levels (i.e., October 2008) and the period with extremely low VIX levels (i.e., March 2013) than during other periods. This could be explained by the fact that the extreme volatilities are "smoothed" by the weighting scheme, resulting in better fitting,

- The majority of the models perform better than the PBS models, which is consistent with the observations we have made using the unweighted scheme.

Cross-referencing the adjusted R^2-statistics using the unweighted scheme, the following conclusions could be drawn:

- Using the weighted scheme, the data appear to fit better to the observed data than using the unweighted scheme, this observation applies to all models, and is independent of the level of VIX index. This should be expected as the weighting scheme essentially gives some smoothing effect to the volatility surface, making polynomial fitting easier,

- Using both the weighted and unweighted schemes, the best two fitting models are Models 7 and 8, even though the third best fitting models are different based on different schemes,

- The models seem to give better fits, in general, for periods with the highest and lowest VIX index levels.

The second statistics analyzed is the RMSE statistics, and the results are summarized in Table 3.15:

Table 3.15: Summary of RMSE Statistics for Models 1 - 8 using Weighted Scheme

Period	Model 1	Model 2	Model 3	Model 4	Model 5	Model 6	Model 7	Model 8
200810	0.214469	0.042741	0.033878	0.028998	0.026122	0.033327	0.023885	0.022745
201005	0.154973	0.039051	0.035671	0.034432	0.027881	0.038745	0.022491	0.025516
201108	0.133558	0.048804	0.042463	0.035240	0.022392	0.038761	0.022841	0.020283
Avg High VIX	**0.167667**	**0.043532**	**0.037337**	**0.032890**	**0.025465**	**0.036944**	**0.023072**	**0.022848**
201208	0.086706	0.033062	0.016805	0.014534	0.016230	0.017658	0.009492	0.012405
201302	0.074095	0.023109	0.010775	0.010069	0.012683	0.019656	0.007487	0.009487
201303	0.078671	0.023988	0.011150	0.010358	0.011752	0.017463	0.007501	0.009394
Avg Low VIX	**0.079824**	**0.026720**	**0.012910**	**0.011654**	**0.013555**	**0.018259**	**0.008160**	**0.010428**

and the RMSE of the benchmark models are reported below in Table 3.16:

Table 3.16: Summary of RMSE Statistics for PBS Models using Weighted Scheme

RMSE	PBSa	PBSb
200810	0.053417	0.052386
201005	0.051551	0.054033
201108	0.054350	0.057257
Avg High VIX	**0.053106**	**0.054559**
201208	0.023670	0.024482
201302	0.025067	0.026416
201303	0.022176	0.023477
Avg Low VIX	**0.023638**	**0.024792**

Based on the results above, we can draw the following conclusions:

- Models 7 and 8 are the best fitting models during both high- and low-VIX periods, whereas Model 5 is the third best performing model during the periods with high VIX index levels. However at low VIX index levels, both Model 4 and Model 3 outperform Model 5, with Model 4 being the third best fitting model,

- Unlike the adjusted R^2-statistics, the RMSE statistics does not show significantly better fitting at extreme values. In fact there is no consistent pattern to indicate the RMSE is smaller during the extreme high and low VIX periods,

- As with the previous statistics, all but Model 1 perform better than the PBS models during both the high and low VIX periods.

Similar to the case of the unweighted scheme, fitted volatility surface plots using the weighted scheme for some of the days during the October 2008 and March 2013 periods are shown. As usual, the plots are using fitted volatilities against simple moneyness and time to maturity in years.

Figure 3.32 is the fitted graph using Model 5 for the October 2008 period, one of the periods with high VIX levels:

Fitted Surface Plot for October 20 - 31, 2008 Using Weighted Scheme with Model 5
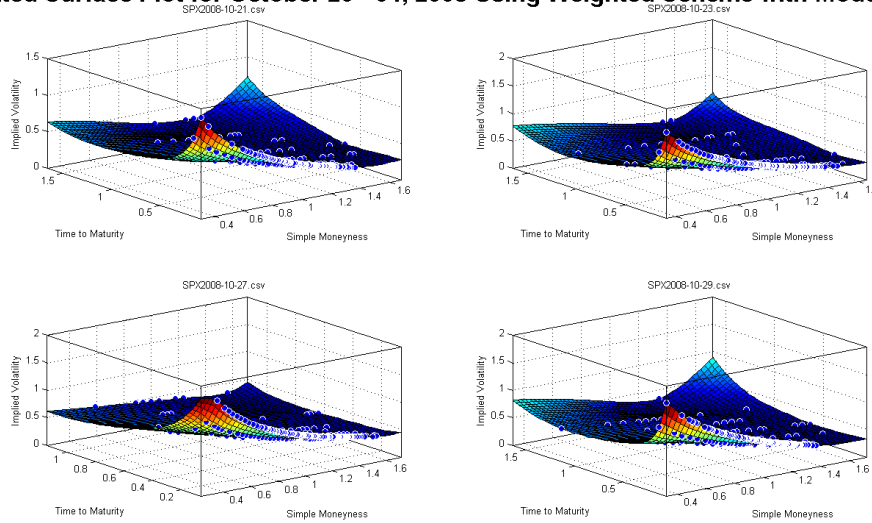

Figure 3.32: Fitted Implied Volatility Surface for October 20-31, 2008 Using Model 5 with Weighted Scheme

and fitted surface using Model 7 for the same period is given in Figure 3.33:

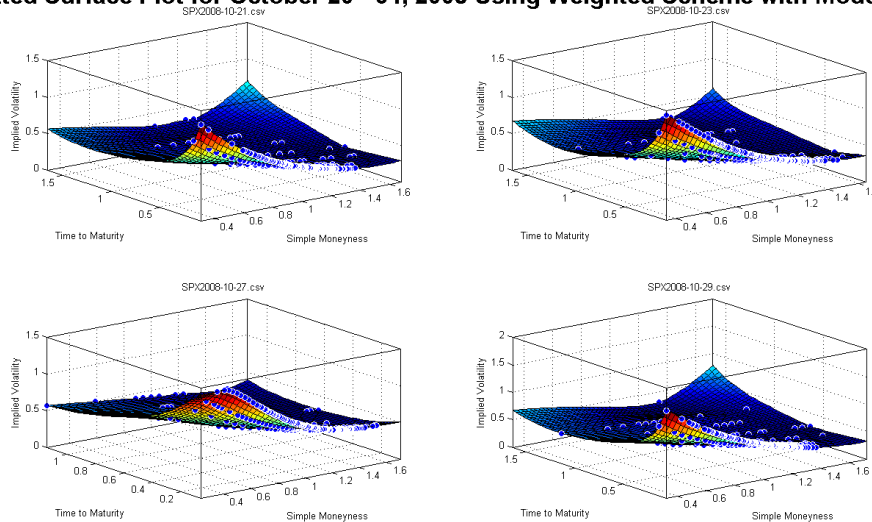**Fitted Surface Plot for October 20 - 31, 2008 Using Weighted Scheme with Model 7**

Figure 3.33: Fitted Implied Volatility Surface for October 20-31, 2008 Using Model 7 with Weighted Scheme

There is very little difference between Figure 3.32 and Figure 3.33. However, during

the low VIX period, the differences are more visible:

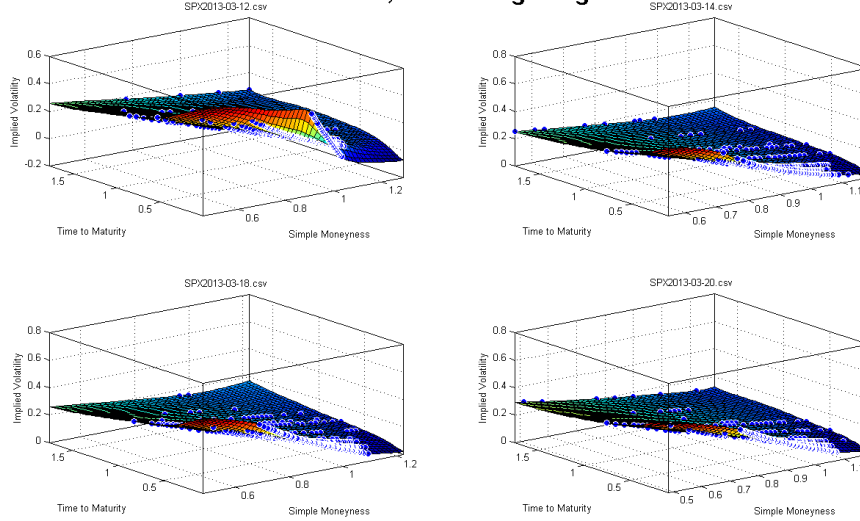**Fitted Surface Plot for March 11-22, 2013 Using Weighted Scheme with Model 5**

Figure 3.34: Fitted Implied Volatility Surface for March 11-22, 2013 Using Model 5 with Weighted Scheme

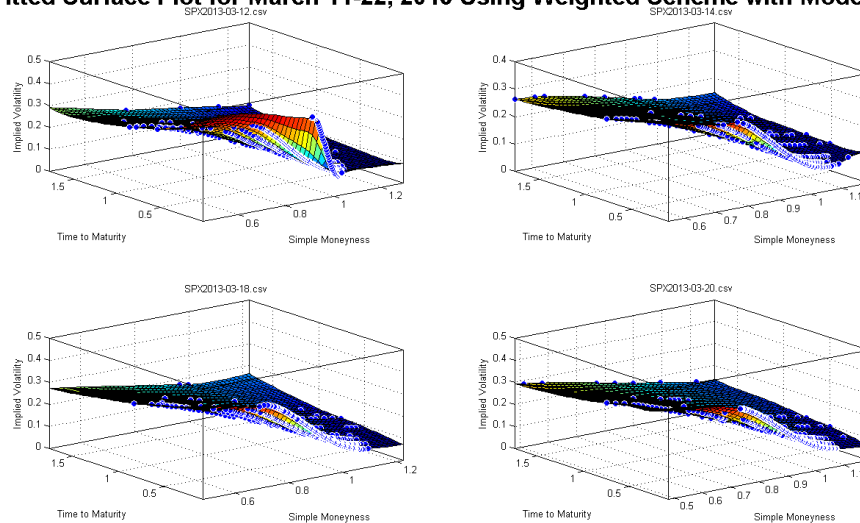**Fitted Surface Plot for March 11-22, 2013 Using Weighted Scheme with Model 7**

Figure 3.35: Fitted Implied Volatility Surface for March 11-22, 2013 Using Model 7 with Weighted Scheme

Comparing the two plots using the data during the March 2013 period, the fitted volatility surfaces with Model 7 (i.e., Figure 3.35) have produced an upward skew which is closer the observed volatility surface. The fitted surfaces produced by Model 5 (i.e.,

Figure 3.34) have once again showed a downward skew, which is less than ideal.

3.6.4 Residual analysis using weighted fitting scheme

The residuals using the weighted scheme for both periods are also analyzed and the plots for the relevant periods are shown here. Figure 3.36 and 3.37 use the data in the October 2008 period, with a high level of VIX index, applying Models 5 and 7 respectively:
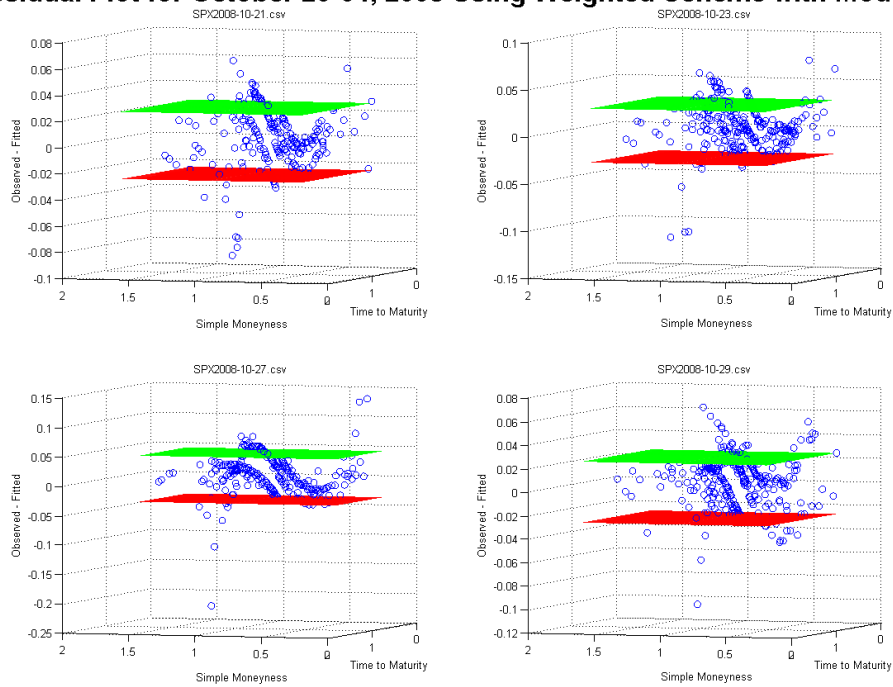

Figure 3.36: Residual Plot for October 20-31, 2008 Using Model 5 with Weighted Scheme

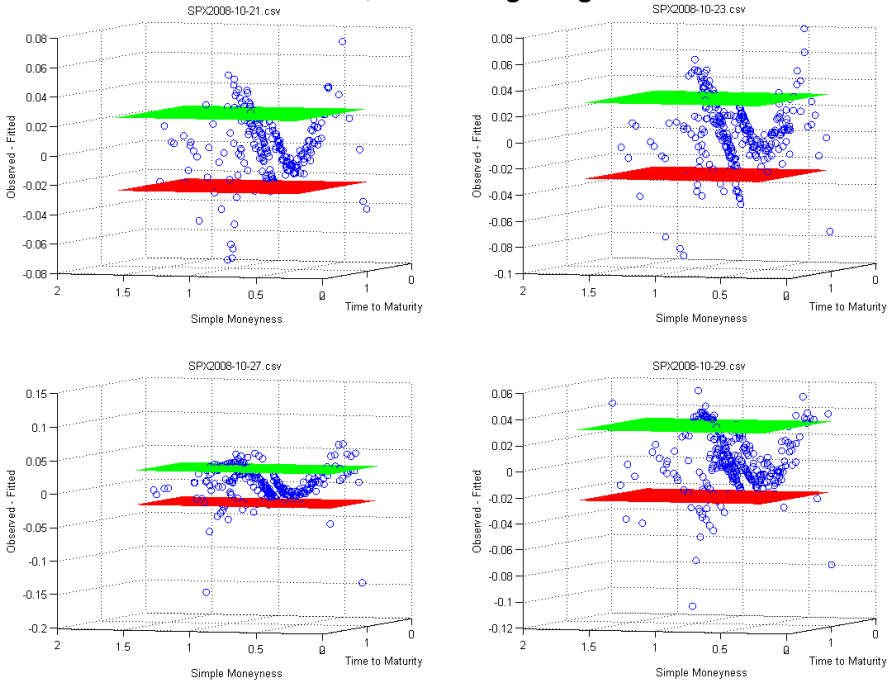**Residual Plot for October 20-31, 2008 Using Weighted Scheme with Model 7**

Figure 3.37: Residual Plot for October 20-31, 2008 Using Model 7 with Weighted Scheme

Comparing to the same plot produced using the unweighted scheme, other than the fact that the largest residuals appear to be a little smaller than before, there is no obvious change in the pattern of the residual plot. The same is observed with the plot for the days in March 2013 period, which has relatively low VIX index levels:

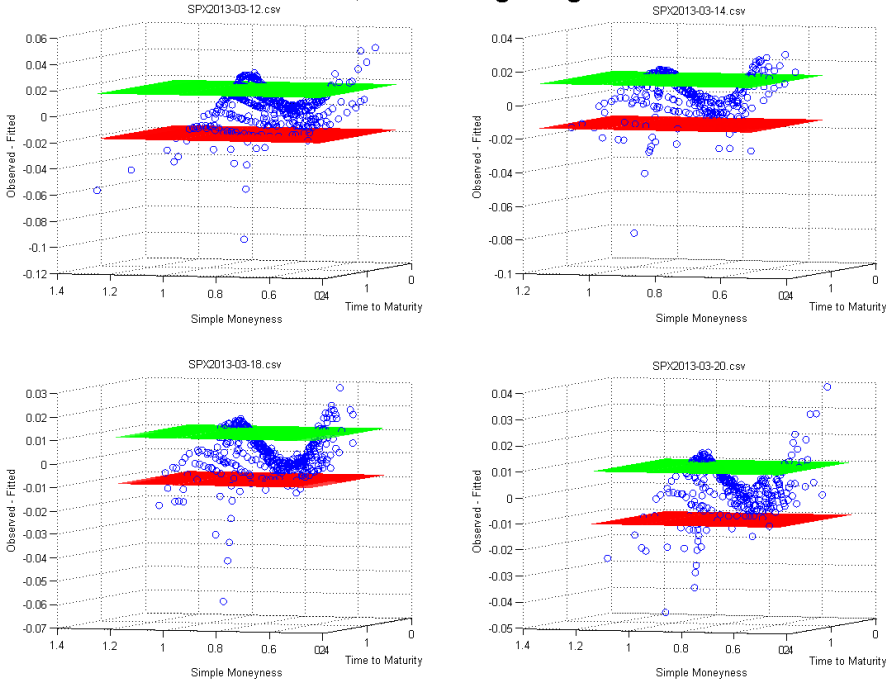**Figure 3.38: R**esidual Plot for March 11-22, 2013 Using Model 5 with Weighted Scheme
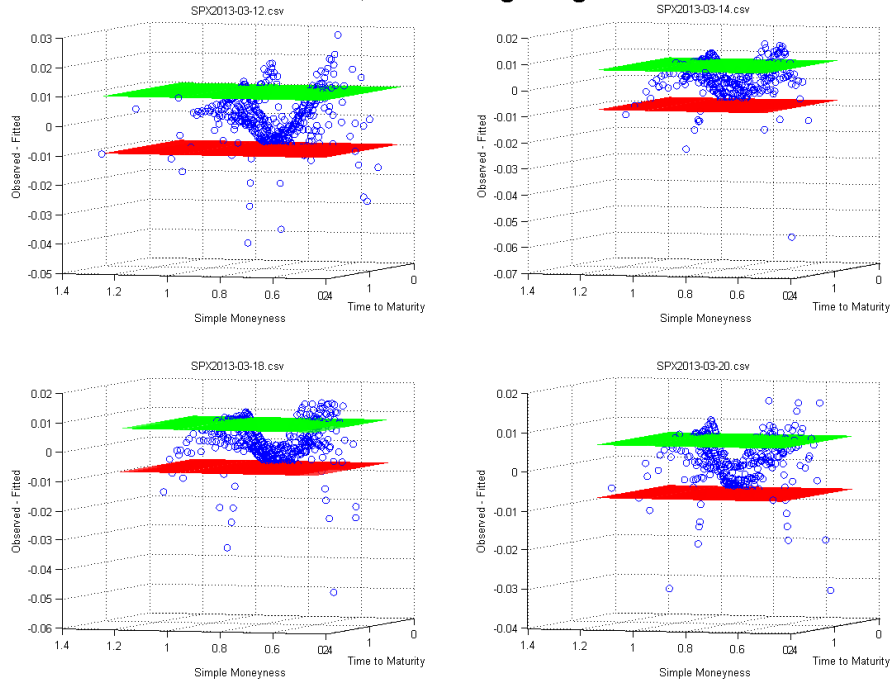
Figure 3.39: Residual Plot for March 11-22, 2013 Using Model 7 with Weighted Scheme

As the residual plot is similar to the plot generated by using the unweighted scheme, we reach a similar conclusion to the case of the weighted scheme, i.e., the residuals of the fitted surfaces generated using Model 7 shows smaller variance compared to the residuals of the surfaces generated using Model 5.

Therefore, overall, Model 7 appears to give a better fit to the observed volatility surfaces than what Roux has originally proposed. Quantitatively it gives higher adjusted R^2-statistics and smaller RMSE values in general compared to the specification proposed by Roux. Observing the plots we have also noticed improvements in fitting the observed volatility surface by using Model 7, most notably in terms of producing the observed volatility smile rather than skew and also of giving rise to more acute curvatures near at-the-money strike prices.

Chapter 4

Conclusion

This thesis has focused on the parametric regression representation of the implied volatility surface of the S&P 500 index options, during our unusual sample periods which is characterized by episodes before, during and after the global financial crisis, using the overnight USD-LIBOR rate as the risk-free interest rate. The VIX index, which is the weighted average of the implied volatilities of S&P 500 index options at various strike levels, is also used both as a factor in some parametric regression models and as an indicator of the periods of high and low market volatility.

As we have observed through the reported empirical analysis performed in this thesis, quadratic polynomials using time to maturity and moneyness as factors may not be sufficient in representing the variations in the implied volatilities. Therefore we proposed several models involving third degree polynomials.

Model 6, which is the first model presented in this thesis, is a third degree polynomial and a function of simple moneyness and time to maturity, with two variations modelling the implied volatility itself and the residual of the implied volatility after subtracting VIX index respectively:

Model 6a: $\sigma_t(m_t, \tau_t) = p_{00,t} + p_{10,t}m_t + p_{01,t}\tau_t + p_{20,t}m_t^2 + p_{11,t}m_t * \tau_t + p_{02,t}\tau_t^2 + p_{30,t} * m_t^3 + p_{21,t} * m_t^2 * \tau_t + p_{12,t} * m_t * \tau_t^2 + p_{03,t} * \tau_t^3 + \epsilon$

Model 6b: $\sigma_t(m_t, \tau_t) - VIX_t = p_{00,t} + p_{10,t}m_t + p_{01,t}\tau_t + p_{20,t}m_t^2 + p_{11,t}m_t * \tau_t +$

$p_{02,t}\tau_t^2 + p_{30,t} * m_t^3 + p_{21,t} * m_t^2 * \tau_t + p_{12,t} * m_t * \tau_t^2 + p_{03,t} * \tau_t^3 + \epsilon$

Model 7 is derived from Model 6 but uses the implied moneyness:

Model 7: $\sigma_t(M_t, \tau_t) = p_{00,t} + p_{10,t}M_t + p_{01,t}\tau_t + p_{20,t}M_t^2 + p_{11,t}M_t * \tau_t + p_{02,t}\tau_t^2 + p_{30,t} * M_t^3 + p_{21,t} * M_t^2 * \tau_t + p_{12,t} * M_t * \tau_t^2 + p_{03,t} * \tau_t^3 + \epsilon$

and Model 8 is similar to the Roux model but has higher degree terms:

Model 8: $\sigma_t(m_t, \tau_t) = p_{00,t} + p_{10,t} * \log(m_t) + p_{01,t} * \frac{1}{\sqrt{\tau_t}} + p_{20,t}(\log(m_t))^2 + p_{11,t}\log(m_t) * \frac{1}{\sqrt{\tau_t}} + p_{02,t}(\frac{1}{\sqrt{\tau_t}})^2 + p_{30,t} * (\log(m_t))^3 + p_{21,t} * (\log(m_t))^2 * \frac{1}{\sqrt{\tau_t}} + p_{12,t} * (\log(m_t)) * (\frac{1}{\sqrt{\tau_t}})^2 + p_{03,t} * (\frac{1}{\sqrt{\tau_t}})^3 + \epsilon$

We have also analyzed the possibility of using promptness, instead of time to maturity, as a factor in the parametric models, particularly in view of the current low interest rate environment. By doing such, although there will be some loss in granularity, the model is more transient and does not require re-calibration on daily basis.

Since this thesis uses the actual S&P 500 index option data, it is also necessary to make some adjustments to the data to ensure only the implied volatilities that are observed due to actual transactions are included, rather than options that are being quoted artificially by the market-makers but are not actually traded. Furthermore, Roux [25] has stated that the rationale for having the weighted scheme is due to the fact that options with high implied volatilities are not actively traded, which may not necessarily be the case from our observations for our sample period.

Least square fitting are used for both the equal-weighted fitting scheme as well as the alternative fitting scheme which uses the observed implied volatility values as the weights.

From the empirical analysis performed in this thesis, we can draw the following conclusions:

- Among all models analyzed, the adjusted R^2-statistics and the RMSE statistics indicate that **Model 7** fits the best during both the high and low stress periods, by using both weighted and unweighted fitting schemes,

- **Model 8** is also a relatively good candidate particularly given the fact that it does not require the implied moneyness to be computed, since implied moneyness is not

only more computationally intensive but also produces unpredictable results when the simple moneyness, m, is close to 0.

Some possible directions for further research include:

- Using an alternative fitting methodology. Other than least-square fitting, it is possible to use some other fitting methodologies such as the Least Absolute Residuals (LAR) method, which is considered as a "robust" fitting method. By using LAR, the absolute differences are minimized rather than the square differences and hence large differences would have less influence on the final results, resulting in more robust fitting.

- Using trading volume as the weighting factor. In essence, the observed implied volatilities is used as a proxy to the trading volume in the weighted scheme that Roux has proposed, and hence it might be better to use trading volume as the weight directly rather than the observed implied volatilities.

- Predictive modelling. A natural step following the analysis of the fitting models would be using the models to predict the future behaviour of implied volatility. Through our preliminary analysis, it appears that even though Model 7 produces good fit results, it is actually lacking behind when predicting the future behaviour of the implied volatility surfaces. Using a rolling five-day scheme (i.e., using the parameters derived by fitting the previous (n-5) trading days of data to predict the implied volatility surface on day n), Model 5 appears to have better prediction power.

In summary, the recent global financial crisis has induced substantial structural changes in the financial markets; as a result they call for renewed specifications of parametric regression representations for the purpose of obtaining more accurate fitting and prediction of the implied volatility surface. This is the task undertaken by this thesis. We believe that the empirical results reported in this thesis have made us closer to fulfilling this task.

Bibliography

[1] A. Alentorn, *Modelling the implied volatility surface: an empirical study for FTSE options*, working paper, 2004

[2] I. U. Badshah, *Modeling the Dynamics of Implied Volatility Surfaces*, working paper, 2009

[3] F. Black, M. Scholes, *The Pricing of Options and Corporate Liabilities*, The Journal of Political Economy, Vol. 81, No. 3 (May - Jun., 1973), pp. 637-654

[4] P. Carr, L. Wu, *A New Framework for Analyzing Volatility Risk and Premium Across Option Strikes and Expiries*, Quantitative Finance Workshop, Kellogg School of Management, Northwestern University, 2012

[5] Chicago Board of Exchange, *The CBOE Volatility Index® - VIX®*, 2009

[6] P. Christoffersen, K. Jacobs, *The Importance of the Loss Function in Option Valuation*, EFA 2003 Annual Conference Paper No. 604, 2002

[7] R. Cont and J. Fonseca *Dynamics of Implied Volatility Surfaces*, Quantitative Finance Vol 2 (2002) 45-60, 2001

[8] J. Cox. *Notes on Option Pricing I: Constant Elasticity of Variance Diffusions*, Working Paper Stanford University, 1975

[9] J. Cox, J. Ingersoll, S. Ross, 1985, *A theory of the term structure of interest rates*, Econometrica 53, 385407

[10] E. Derman, *Regimes of Volatility: Some Observations on the Variation of S & P 500 Implied Volatilities*, Goldman Sachs Quantitative Strategies Research Notes, 1999

[11] E. Derman, I. Kani, *The Volatility Smile and Its Implied Tree*, Goldman Sachs quantitative Strategies Research Notes, 1994

[12] B. Dumas, J. Fleming and R. Whaley, *Implied Volatility Functions: Empirical Tests*,The Journal of Finance, Vol LIII, No. 6, 2059-2106

[13] B. Dupire, *Pricing with Smile*, Risk, 1994

[14] J. Gatheral, *A parsimonious arbitrage-free implied volatility parameterization with application to the valuation of volatility derivatives*, Presentation at Global Derivatives, 2004

[15] J. Gatheral, *Lecture 1: Stochastic Volatility and Local Volatility*, Case Studies in Financial Modelling Course Notes, Courant Institute of Mathematical Sciences, Fall Term, 2002

[16] P. Hagan, D. Kumar, A. Lesniewski, and D. Woodward, *Managing Smile Risk*, Wilmott Magazine (September 2002), 84-108

[17] S. Heston,*A closed-form solution for options with stochastic volatility, with application to bond and currency options*, Review of Financial Studies 6, 327343, 1993

[18] C. Homescu, *Implied Volatility Surface: Construction Methodologies and Characteristics*, working paper

[19] J. Hull, *Option, Futures and other Derivatives*, 8th Edition, 222, Pearson Education Limited, 2012

[20] I.T. Jolliffe, *Principle Component Analysis*, 2nd, Springer, 2002

[21] N. Kahale, *An arbitrage-free interpolation of volatilities*, Risk Magazine, 17:102106, 2004

[22] O. Ledoit, P. Santa-Clara, *Relative Pricing of Options with Stochastic Volatility* (March 1998). University of California-Los Angeles Finance Working Paper 9-98

[23] D. Madan, E. Seneta, *The Variance Gamma (V.G.) Model for Share Market Returns*, The Journal of Business, Vol. 64, No. 4 (Oct. 1990), pp. 511-524, University of Chicago Press

[24] D. Madan, P. Carr, E. Chang, *The Variance Gamma Process and Option Pricing*, European Finance Review 2: 79105, Kluwer Academic Publishers, 1998

[25] M. Roux, *A Long-Term Model of the Dynamics of the S& P 500 Implied Volatility Surface*, North American Actuarial Journal, Volume 11, Number 4,2007

[26] A. Subrahmanyam, *Psychology, ecomomic and financial markets: general Views*, Quantitative Behavioural Finance Conference, University of Waterloo, 2013